© 2014. Published by The Company of Biologists Ltd | Development (2014) 141, 773-783 doi:10.1242/dev.096131

RESEARCH ARTICLE

STEM CELLS AND REGENERATION

Growth/differentiation factor 15 promotes EGFR signalling, and regulates proliferation and migration in the hippocampus of neonatal and young adult mice

Carmen Carrillo-García[1,2], Sebastian Prochnow[2,*], Ina K. Simeonova[1,3], Jens Strelau[2], Gabriele Hölzl-Wenig[1], Claudia Mandl[1], Klaus Unsicker[2,4], Oliver von Bohlen und Halbach[2,5] and Francesca Ciccolini[1,‡]

ABSTRACT

The activation of epidermal growth factor receptor (EGFR) affects multiple aspects of neural precursor behaviour, including proliferation and migration. Telencephalic precursors acquire EGF responsiveness and upregulate EGFR expression at late stages of development. The events regulating this process and its significance are still unclear. We here show that in the developing and postnatal hippocampus (HP), growth/differentiation factor (GDF) 15 and EGFR are co-expressed in primitive precursors as well as in more differentiated cells. We also provide evidence that GDF15 promotes responsiveness to EGF and EGFR expression in hippocampal precursors through a mechanism that requires active CXC chemokine receptor (CXCR) 4. Besides EGFR expression, GDF15 ablation also leads to decreased proliferation and migration. In particular, lack of GDF15 impairs both processes in the cornu ammonis (CA) 1 and only proliferation in the dentate gyrus (DG). Importantly, migration and proliferation in the mutant HP were altered only perinatally, when EGFR expression was also affected. These data suggest that GDF15 regulates migration and proliferation by promoting EGFR signalling in the perinatal HP and represent a first description of a functional role for GDF15 in the developing telencephalon.

KEY WORDS: GDF15, EGFR, Hippocampus, Neurogenesis, Migration, Proliferation, Mouse

INTRODUCTION

The hippocampus (HP) is involved in key functions such as learning, memory and the regulation of sexual and emotional behaviour. At least six separate regions can be identified in the adult HP, with the dentate gyrus (DG) and the cornu ammonis (CA) being the most characterised. The CA derives from precursors located in the ammonic neuroepithelium, whereas the DG is established through sequential migrations, leading to the generation of a secondary radial glia scaffold and the relocation of neural precursors from the primary dentate epithelium into the DG area (Altman and Bayer, 1990; Li and Pleasure, 2005). Like most hippocampal projection neurons, CA pyramidal cells are formed before birth. By contrast, the generation of granule cells in the DG begins shortly before birth and continues postnatally. In the adult HP, appreciable neurogenesis occurs only in the subgranular zone (SGZ) of the DG (Cameron et al., 1993; Ehninger and Kempermann, 2008). However, neural precursors may also be present in the CA region within the hippocampal subependyma (Chechneva et al., 2005; Rietze et al., 2000).

From late development onwards, the expression of epidermal growth factor receptor (EGFR) is increased in neural precursors in the CA1 and to a lesser extent in the DG (Carrillo-García et al., 2010). Although these EGFR^{high} precursors include cells displaying *in vitro* characteristics of stem cells, their number rapidly decreases after birth (Carrillo-García et al., 2010). Despite this, EGFR is expressed in proliferating precursors in the adult SGZ (Okano et al., 1996) and EGF promotes proliferation *in vitro* and *in vivo* in both the adult CA1 and DG (Becq et al., 2005; Nakatomi et al., 2002). Moreover, EGFR is also expressed in adult CA neurons (Tucker et al., 1993), suggesting that EGFR signalling may regulate additional processes in the adult HP.

Few signals have been involved in the regulation of EGFR expression in neural precursors. For example, fibroblast growth factor (FGF) 2 and bone morphogenetic protein (BMP) 4 have been shown to promote and downregulate EGFR expression in cultured neural precursors, respectively (Ciccolini and Svendsen, 1998; Lillien and Raphael, 2000). In addition, stromal-derived factor (SDF) 1 modulates EGFR expression in adult EGFR^{high} cells, thereby affecting their ability to migrate in a CXC chemokine receptor (CXCR) 4-dependent manner (Kokovay et al., 2010).

In adult rodents, growth/differentiation factor (GDF) 15, a member of the transforming growth factor β super family, is expressed in several organs and tissues, including in the developing and adult rat brain, albeit at lower levels than in other tissues (Böttner et al., 1999). In the neonatal rat brain, GDF15 is expressed not only in ependymal cells but also in the underlying germinal epithelium (Schober et al., 2001), suggesting that it may affect the behaviour of neural precursors. Indeed, we here provide evidence that lack of GDF15 affects EGFR signalling in hippocampal precursors. Moreover, we found that also migration and proliferation are altered in the mutant HP, albeit only in concomitance with defective EGFR expression.

[1]Department of Neurobiology, Interdisciplinary Centre for Neuroscience (IZN), Ruprecht-Karls University of Heidelberg, Im Neuenheimer Feld 364, D-69120 Heidelberg, Germany. [2]Department of Neuroanatomy, Interdisciplinary Centre for Neurosciences (IZN), Ruprecht-Karls University of Heidelberg, Im Neuenheimer Feld 306, D-69120 Heidelberg, Germany. [3]Spinal Cord Injury Center, Heidelberg University Hospital, Schlierbacher Landstrasse 200a, D-69118 Heidelberg, Germany. [4]Department of Molecular Embryology, Institute of Anatomy & Cell Biology, Albert-Ludwigs University of Freiburg, Albertstrasse 17, D-79104 Freiburg, Germany. [5]Institute of Anatomy and Cell Biology, Ernst Moritz Arndt Universitätsmedizin Greifswald, Friedrich-Loeffler-Strasse 23c, D-17487 Greifswald, Germany.
*Present address: Universitätsklinikum Hamburg-Eppendorf, Martinistrasse 52, 20246 Hamburg, Germany.

‡Author for correspondence (f.ciccolini@uni-hd.de)

Received 6 March 2013; Accepted 11 November 2013

Development (2014) doi:10.1242/dev.096131

RESULTS

GDF15 is expressed in neural precursors

Previous studies have shown that GDF15 is expressed in the choroid plexus and in the subependymal region surrounding the lateral ventricle (Schober et al., 2001; Strelau et al., 2000). However, its expression in the murine telencephalon has not yet been investigated. Therefore, we first took advantage of quantitative real time PCR (qPCR) to quantify levels of *Gdf15* mRNA in the developing (E14-E18) and adult (P48) cortex (Ctx) and HP, as well as in the germinal zone lining the embryonic ganglionic eminence (GE) (Ciccolini and Svendsen, 2001) and the adult lateral ventricle (lSEZ) (Fig. 1A). Transcripts for *Gdf15* were detected in all regions at all ages. From E16 onwards, *Gdf15* mRNA was more abundant in both the GE/lSEZ and HP than in the age-matched cortical tissue. Consistent with the possibility that *Gdf15* is expressed in neural precursors, in the embryonic telencephalon the highest levels of *Gdf15* expression were observed in the HP at E14 (Fig. 1A), before the emergence of the pyramidal layer, when most of the hippocampal formation consists of the ventricular zone (Soriano et al., 1994), whereas in the adult telencephalon, *Gdf15* transcripts were most abundant in the lSEZ (Fig. 1A). To further investigate *Gdf15* expression in neural precursors, we next sorted EGFR^{high} cells from the dissociated E18 HP and GE using flow cytometry, as we have previously shown that in both regions this cell population is highly enriched in self-renewing and multipotent precursors (Carrillo-García et al., 2010; Ciccolini et al., 2005). Both EGFR^{high} cells isolated from the HP and especially from the GE (Fig. 1B) contained significantly more *Gdf15* mRNA than the respective EGFR^{low} populations. To directly test whether *Gdf15*-expressing cells display stem cell activity, we took advantage of mice in which the two exons of the *Gdf15* gene have been replaced by the bacterial β-galactosidase (LacZ) gene (*Gdf15*$^{-/-}$) (Strelau et al., 2009). In these experiments, we also analysed either EGFR or prominin expression as they are expressed in different subsets of clonogenic precursors: whereas prominin labels embryonic radial glia cells and postnatal neural stem cells both in the lSEZ and in the HP (Beckervordersandforth et al., 2010; Walker et al., 2013), EGFR is mainly associated with intermediate precursors (Ciccolini et al., 2005). In fact, in the postnatal lSEZ few EGFR^{high} cells express stem cell markers and most represent clonogenic transit-amplifying precursors (TAPs) and non-clonogenic pre-neuroblasts (Cesetti et al., 2009). For this analysis, cells dissociated from the E18 HP and GE were exposed to a hypo-osmotic solution before sorting, to allow the entry of the fluorescent LacZ substrate. As this procedure leads to an increase in the expression of EGFR at the cell surface (Cesetti et al., 2011), it also allows the collection within the EGFR^{high} fraction of those cells that, under normal osmotic conditions, express only intermediate EGFR levels. Consistent with our previous analysis, in both telencephalic regions more LacZ^{+} cells were present within the EGFR^{high} than in the EGFR^{low} population (supplementary material Fig. S1A). In the HP, LacZ^{+} cells were also more abundant in the prominin^{+} than in the prominin^{-} population (supplementary material Fig. S1C). A similar trend was observed in the GE, albeit it was not significant (supplementary material Fig. S1C). Analysis of the clonogenic activity also indicated differences between the populations isolated from the two telencephalic regions. In the HP, the incidence of clonogenic LacZ^{+} cells was higher in prominin^{+} than in EGFR^{high} cells (supplementary material Fig. S1, compare B with D), whereas the opposite was observed in the GE (supplementary material Fig. S1, compare B with D). Thus, in both telencephalic regions *Gdf15* is expressed in clone-forming precursors. However, whereas in the HP these clonogenic precursors express the stem cell marker prominin, in the GE they predominantly display an antigenic profile of TAPs.

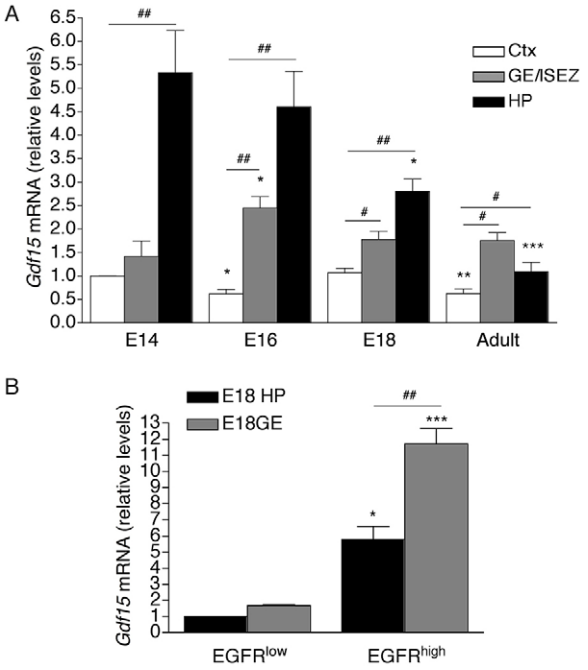

Fig. 1. Expression of *Gdf15* transcripts in the developing telencephalon. Levels of *Gdf15* transcripts in the indicated developing and adult telencephalic regions (A), and in EGFR^{low} and EGFR^{high} cells isolated from the indicated regions of the E18 telencephalon by FACS (B). Values represent levels of *Gdf15* relative to *18s* rRNA (A) and to *Gadph* and β-Actin mRNAs (B) after normalization to the E14 cortical tissue (A) and hippocampal EGFR^{low} cells (B). E, embryonic day; GE, ganglionic eminence; HP, hippocampus. Ctx, cortex; lSEZ, lateral subependymal zone. * and # indicate values that are significantly different from the corresponding E14 tissue and age-matched cortical tissue, respectively. *,#P≤0.05; **,##P≤0.01; ***P≤0.001; n≥5.

We next investigated GDF15 expression in coronal hippocampal sections obtained from 2-month-old mice. Confirming the specificity of the immunostaining, GDF15 immunoreactivity was observed in close proximity of the nucleus in permeabilized wild-type, but not in mutant slices (supplementary material Fig. S2). In the DG, GDF15^{+} cells were mainly present in the SGZ (supplementary material Fig. S2Ab), showing that GDF15 is expressed in neural precursor cells also in the adult HP. By contrast, in the CA1, GDF15^{+} cells were almost exclusively located within the pyramidal cell body layer (supplementary material Fig. S2Aa). Double immunostaining with GDF15 and EGFR (Fig. 2A,B), GFAP (Fig. 2C,D) or nestin (Fig. 2E,F) antibodies confirmed the different pattern of GDF15 expression in the hippocampal subregions. In the CA1, GDF15 and EGFR were extensively co-expressed within the pyramidal cell body layer (Fig. 2A), whereas very rare GDF15^{+}/GFAP^{+} (Fig. 2C) and virtually no GDF15^{+}/Nestin^{+} (Fig. 2E) cells were detected. By contrast, GDF15^{+}/GFAP^{+} (Fig. 2D) and GDF15^{+}/nestin^{+} (Fig. 2F) cells were present in the DG. Colocalization of GDF15 and EGFR was observed also in the SGZ (Fig. 2Bb‴, arrowheads), albeit to a lower extent than in the CA1. Interestingly, in the DG a few EGFR^{+}/GDF15^{+} cells were present in the granule zone just above the germinal area, suggesting that they represent young granule neurons (Fig. 2B, arrows). Thus, in both the

Development (2014) doi:10.1242/dev.096131

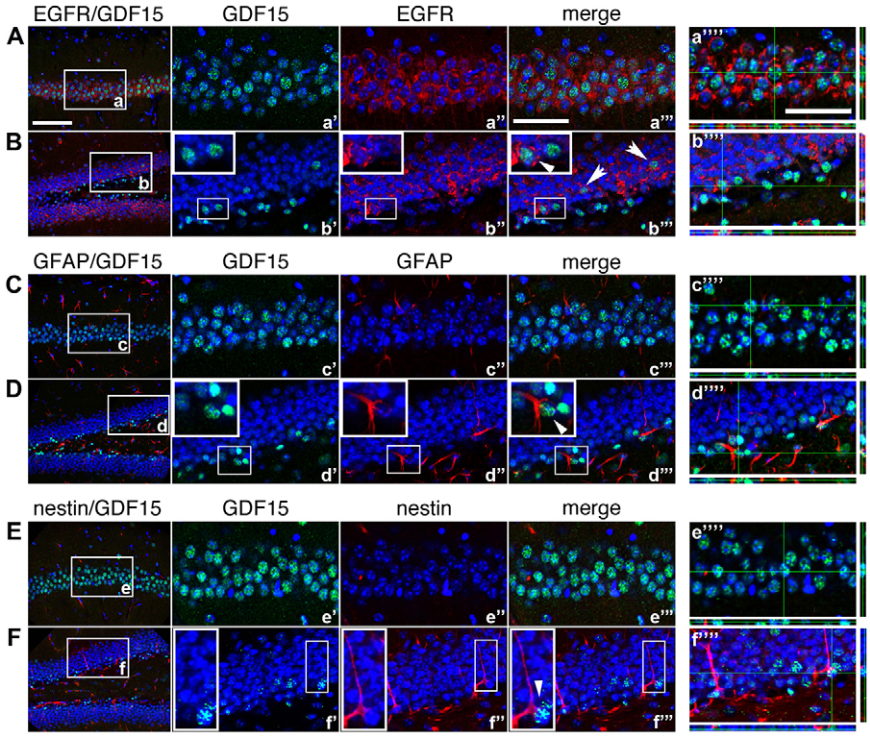

Fig. 2. Characterization of GDF15 expressing cells in the adult HP. Representative photomicrographs illustrating GDF15 (green) and EGFR (A,B), GFAP (C,D) or nestin (E,F) (red) immunoreactivity and DAPI counterstaining of the nuclei (blue) in the CA1 (A,C,E) and the DG (B,D,F) after double immunostaining of coronal hippocampal sections. Higher magnifications of boxed areas are shown in the green (a′-f′), in the red (a″-f″) channels and as merge (a‴-f‴). Orthogonal views relative to double immunostained cells are shown in the right column (a⁗-f⁗). Scale bars: 100 µm (left column); 50 µm for the higher magnification panels (all from a′-f′ to a⁗-f⁗).

developing and postnatal HP, GDF15 is expressed in neural precursors as well as in more differentiated cells.

Decreased EGFR expression and signalling in the E18 *Gdf15*$^{-/-}$ HP

We next investigated whether lack of *Gdf15* affects precursor behaviour. We first analysed the ability of wild-type and mutant precursors to proliferate *in vitro* by means of neurosphere assays. After one week in the presence of exogenous EGF and FGF2, neurosphere cultures established from the dissociated E18 *Gdf15*$^{-/-}$ HP contained significantly fewer cells than the wild-type counterpart (Fig. 3A). This difference was not due to an effect of the genotype on the number of neurosphere-forming cells or cell viability, as shown by clonal assays (Fig. 3B) and PI exclusion (supplementary material Table S1), respectively. It was also not due to a mitogenic effect of GDF15, as the presence of the exogenous growth factor did not affect cell numbers after one week in culture (Fig. 3A). Together, these data indicate that mutant E18 precursors display a reduced proliferation potential. Therefore, we next investigated whether this change reflected an altered response to EGF and/or FGF2. We have previously shown that the responsiveness to EGF increases during development and EGF and/or FGF2 elicit a similar proliferative response in E18 precursors (Ciccolini, 2001). However, unlike the wild-type counterpart, proliferation was decreased in mutant neurospheres grown in the presence of EGF, with or without FGF2, but not in FGF2 only (Fig. 3C). Interestingly, maximum impairment of proliferation was observed upon culturing with both mitogens, indicating that EGF and FGF2 may interact in regulating precursor proliferation. Consistent with the hypothesis that the impairment of proliferation in mutant precursors depends on altered EGFR signalling, the genotype did not affect proliferation of neurospheres derived from the E14 HP (Fig. 3D), as at this age neural precursors lack responsiveness to EGF (Ciccolini, 2001; Ciccolini and Svendsen, 1998). Taken together, these data show that mutant E18 hippocampal precursors display an altered response to EGF.

Levels of EGFR affect the ability of neural precursors to respond to EGF and the type of response elicited by EGF. Therefore, we next quantified the number of EGFR^{high} cells in the dissociated HP of E18 wild-type and *Gdf15*$^{-/-}$ mice. This analysis revealed that, compared with the wild-type counterpart, the *Gdf15*$^{-/-}$ HP contained fewer EGFR^{high} cells (Fig. 3, compare E and F, see also G). The genotype instead did not affect clone formation (Fig. 3H), proliferative potential and self-renewal of EGFR^{high} cells, or the number of EGFR^{low} cells and their ability to form clones and self-renew (Fig. 3E,F; supplementary material Table S1; data not shown). Quantitative analysis of the mRNAs for *Fgf2*, *Fgfr1* and *Fgfr2*, the main FGF2 receptors expressed in the brain (Maric et al., 2007; Raballo et al., 2000; Saarimäki-Vire et al., 2007), revealed no major differences in transcript levels between wild-type and *Gdf15*$^{-/-}$ embryos (supplementary material Fig. S3A). Moreover, overnight treatment of hippocampal precursors with exogenous FGF2 (Ciccolini and Svendsen, 1998; Lillien and Raphael, 2000; Santa-Olalla and Covarrubias, 1999) increased EGFR expression in mutant cultures to wild-type levels (Fig. 3G), showing that, in the absence of exogenous EGF, FGF2 can rescue both proliferation and EGFR expression in mutant precursors. Treatment with exogenous GDF15 and/or FGF2 similarly increased the number of EGFR^{high} cells in mutant cultures (supplementary material Fig. S3B), indicating that GDF15 also promotes EGFR expression. Concomitant blockade of CXCR4 with AMD3100 prevented the increase in EGFR expression induced by either growth factor treatment for 6 hours without affecting cell viability and levels of EGFR expression in control culture not exposed to exogenous growth factors (supplementary material Fig. S3C; data not shown). A similar effect of CXCR4 inhibition on EGFR expression was observed in GDF15 but not in FGF2-treated cultures after 24 hours (supplementary material Fig. S3D). In summary, these data indicate that GDF15 promotes EGFR expression and EGF responsiveness in E18 hippocampal precursors, and that this effect requires activation of CXCR4.

Development (2014) doi:10.1242/dev.096131

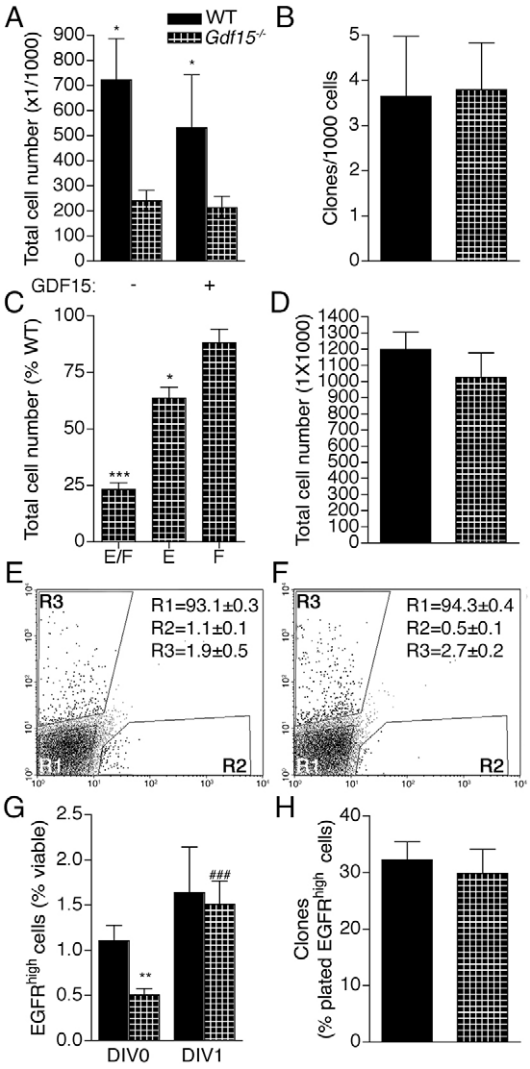

Fig. 3. GDF15 promotes the response to EGF and EGFR expression in hippocampal precursors. (A-D) Quantitative analysis of the total cell number (A,C,D) and clones (B) obtained upon plating E18 (A-C) and E14 (D) wild-type and *Gdf15*$^{-/-}$ cells in both EGF (E) and FGF2 (F) (A,B,D), or E and/or F, as indicated (C). In A, exogenous GDF15 was added as shown. In C, values are the percentage variation of the total cell number scored in parallel wild-type cultures grown in both growth factors. (E,F) Representative dot plots of dissociated E18 wild-type (E) and *Gdf15*$^{-/-}$ (F) HP after staining with EGF-Alexa 488 and PI to reveal EGFR^{low} (R1), EGFR^{high} (R2) and dead cells (R3). Values represent the means±s.e.m. of the percentage of total cells in each gate. (G,H) Quantitative analysis of the EGFR^{high} cell numbers in the E18 wild-type and *Gdf15*$^{-/-}$ HP measured at day *in vitro* (DIV) 0, or after 24 hours exposure to FGF2 (DIV 1) (G) and of the percentage of E18 wild-type and *Gdf15*$^{-/-}$ EGFR^{high} cells capable of undergoing clone formation upon plating at DIV0 (H). * and # indicate values that are significantly different from the corresponding wild-type samples and the counterpart at DIV0, respectively. *P≤0.05; **P≤0.01; ***,###P≤0.001; n≥3.

We next investigated EGFR expression on coronal sections of the wild-type and mutant HP. Independent of the genotype, most EGFR^{+} cells were located in the CA1 and very little immunoreactivity was present in the hippocampal migratory stream and in the prospective DG (Fig. 4), as previously reported (Carrillo-García et al., 2010). However, in both mutant regions the number of EGFR^{+} cells was significantly lower than in the wild-type counterpart (Fig. 4B-D). Independent of the mutation, EGFR^{high} cells expressed significantly higher levels of *Egfr* transcripts than corresponding EGFR^{low} cells (Fig. 4E), which is consistent with previous observations (Carrillo-García et al., 2010). However, compared with the *Gdf15*$^{+/-}$ counterpart, *Egfr* transcripts were reduced in LacZ^{+}/EGFR^{high} cells sorted from the HP of E18 *Gdf15*$^{-/-}$ embryos (Fig. 4E), suggesting that GDF15 regulates EGFR expression only in those cells that express GDF15. This conclusion is apparently at odds with our previous finding that GDF15 mutation leads to a 50% reduction in the number of EGFR^{high} cells (Fig. 3G), as we detected LacZ expression in only 10% of the EGFR^{high} cells isolated from *Gdf15*$^{-/+}$ embryos (supplementary material Fig. S1A). However, this discrepancy is probably due to the hypo-osmotic treatment necessary for the detection of LacZ, which artificially increases the number of EGFR^{high} cells (Cesetti et al., 2011). Thus, absence of GDF15 leads to a reduction in EGFR expression in the E18 HP.

Lack of GDF15 affects precursor proliferation and migration

We have previously observed that most mitotic cells in the E18 HP express EGFR (Carrillo-García et al., 2010). Therefore, we next examined whether GDF15 affects proliferation *in vivo* by quantifying the cells undergoing mitosis in the E18 wild-type and *Gdf15*$^{-/-}$ HP. Double immunostaining with PHH3 and EGFR antibodies revealed that both EGFR^{+} and EGFR^{-} mitotic cells were similarly reduced in the mutant CA1 (Fig. 5A,B). By contrast, in the mutant DG mitosis was significantly reduced only within the population of EGFR^{+} cells (Fig. 5A,C), establishing in this subregion a direct link between the effect of GDF15 on EGFR expression and cell proliferation. Interestingly, the effect of the genotype on the number on EGFR^{+}/PHH3^{+} cells was almost a 50% reduction, similar to the effect of *Gdf15* ablation on the number of EGFR^{high} cells (see for comparison Fig. 3G), and significantly greater than the effect on the total number of EGFR^{+} cells (see for comparison Fig. 4B). This is likely due to the fact that EGFR immunostaining labels all EGFR^{+} cells, whereas EGFR^{high} cells represent only the fraction expressing high levels of EGFR at the cell membrane, which is enriched in rapidly proliferating precursors (Cesetti et al., 2009). We next investigated whether the decrease in proliferation reflected a reduction in the number of dividing cells or a change in cell cycle dynamics. To this end, we administered BrdU to heterozygous E18 time-mated mice and sacrificed them after 2 and 6 hours (Fig. 5D,E). Analysis at 2 hours showed a decreased number of BrdU^{+} in the mutant CA1 but not in the DG. Moreover, comparison of the ratios between the number of BrdU^{+} and PHH3^{+} cells indicated a significant effect of the genotype on cell cycle dynamics in the DG (wild type 6.5±1.9 versus *Gdf15*$^{-/-}$ 10.8±3.2; *P≤0.05) but not in the CA1 (wild type 5.6±0.3 versus *Gdf15*$^{-/-}$ 6.3±0.4). These data indicate that the reduction in the number of mitotic cells reflects in the mutant CA1 a decrease in the number of proliferating precursors and in the mutant DG fewer cells entering mitosis at any given time. Consistent with this hypothesis, 6 hours after BrdU injection the number of BrdU^{+} cells in the mutant DG was significantly reduced (Fig. 5E).

Interestingly, in the wild-type CA1 the length of the chase did not affect the number of BrdU^{+} cells, whereas in the mutant counterpart the number of BrdU^{+} cells increased over time (Fig. 5D). In fact, 6 hours after injection, significantly more BrdU^{+} cells were present in the mutant than in the wild-type CA1, suggesting that lack of *Gdf15* leads to an accumulation of dividing cells in the CA1. Indeed, it is well known that in the perinatal CA1 neural precursors are not sedentary but migrate extensively to the surrounding regions (Navarro-Quiroga et al., 2006). Migration is also involved in the

Development (2014) doi:10.1242/dev.096131

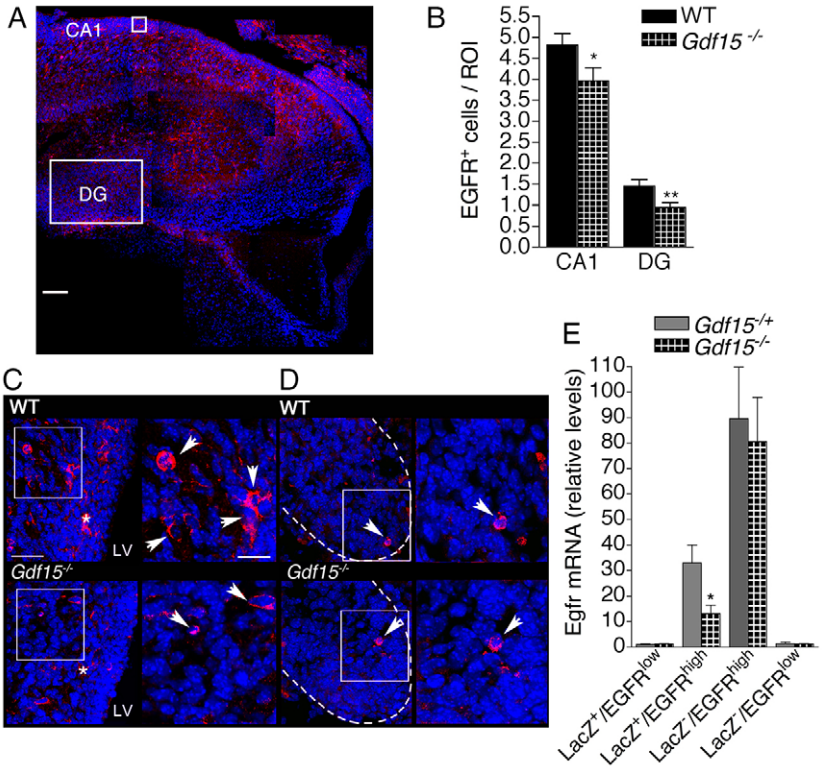

Fig. 4. Decreased EGFR expression in the E18 *Gdf15*$^{-/-}$ HP. (A,C,D) Collage of micrographs of a wild-type coronal section (A) and micrographs of the CA1 (C) and of the DG (D) of wild-type and *Gdf15*$^{-/-}$ embryos as indicated, illustrating representative examples of EGFR immunoreactivity (red) and DAPI nuclear counterstaining (blue). Arrows indicate EGFR^{+} cells (asterisk indicates blood vessels). In A, enclosed squares indicate the regions of interest (ROI) used for the quantification of immunopositive cells shown in B. Scale bar: 75 µm. (E) Expression of *Egfr* transcripts in the indicated *Gdf15*$^{+/-}$ and *Gdf15*$^{-/-}$ cell populations isolated by FACS on the basis of LacZ and EGFR expression. Values represent measurements of *Egfr* relative to *Gadph* and β-Actin mRNAs after normalization to the mRNA levels in the heterozygous LacZ^{+}/EGFR^{low} population. * indicates values significantly different from the wild type (B) and the *Gdf15*$^{+/-}$ (E) counterparts. *P≤0.05; **P≤0.01; n≥4.

relocation of progenitors from the primary dentate epithelium to the forming DG and this process involves activation of CXCR4 receptor (Choe and Pleasure, 2012). However, a similar analysis in the primary dentate epithelium showed no effect of the genotype on the number of BrdU^{+} cells at either time-point (data not shown). This suggests that migration from this germinal zone to the DG is not affected. Indeed, analysis of GFAP, Prox1, NeuroD and Olig2 expression in the DG revealed no gross structural alterations in the forming mutant DG (supplementary material Fig. S4). Therefore, we next investigated cell migration in the wild-type and mutant CA1. We first analysed migration by carefully placing DiI-loaded beads at the apical border of the CA1 in coronal slices of the E18 wild-type HP (Fig. 6). After 3 days *in vitro*, the slices were fixed and the phenotype of DiI-labelled cells was analysed by immunostaining. We found that cells had migrated from the beads both in a tangential direction along the CA subregion and radially reaching the hippocampal fissure (Fig. 6). The majority of the migratory cells expressed EGFR (Fig. 6B), supporting the hypothesis that EGFR expression regulates migration of neural precursors. In addition, some of these cells, including those that had migrated close to the hippocampal fissure, were still undergoing mitosis (Fig. 6A). Many of the DiI-labelled cells expressed glutamate decarboxylase (GAD) 67 and to a lesser extent γ-aminobutyric acid (GABA), indicating that they include interneuron progenitors (supplementary material Fig. S5). This is consistent with the dynamics of interneuron migration in the developing HP (Tricoire et al., 2011). Thus, migratory cells in the E18 CA1 express EGFR and at least some of these cells have not yet exited the cell cycle and undergone terminal differentiation.

We next investigated the effect of GDF15 on migration. This analysis was carried out at postnatal day (P) 0 because the bigger size of the slices allowed a more precise positioning of the beads and EGFR expression is upregulated in the wild-type HP at least until P7 (Carrillo-García et al., 2010). Measurement of the distance between the DiI-loaded beads and the most distal tangentially orientated DiI-labelled cells revealed that within 3 days wild-type cells had migrated a longer distance than their *Gdf15*$^{-/-}$ counterparts (Fig. 7B). As already observed at E18, rare DiI-labelled cells were also present around the hippocampal fissure and in very rare occasions in the DG. Although, owing to their rarity, we could not clearly define their migratory route, within 3 days fewer cells had migrated to this area in mutant than in wild-type slices (Fig. 7C). Thus, lack of GDF15 impairs proliferation and migration in the developing HP.

Impairment of neurogenesis in the postnatal *Gdf15*$^{-/-}$ DG

Our data indicate that deletion of *Gdf15* leads to an impairment of both proliferation and migration in the developing HP. They also suggest that GDF15 exerts this dual regulation by promoting EGFR signalling in neural precursors and that this effect requires CXCR4 activation. We have previously shown that the number of EGFR-expressing precursors in the postnatal HP rapidly declines after birth (Carrillo-García et al., 2010). Therefore, we reasoned that age might attenuate the differences in EGFR expression between the wild-type and mutant HP, thereby allowing us to test the effect of the mutation on proliferation and migration in the absence of altered EGFR expression. We first determined the number of EGFR^{high} cells in each region of the wild-type and mutant HP using differential dissection and FACS analysis, as previously described (Carrillo-García et al., 2010). Consistent with the fact that EGFR expression declines in the aging HP, independent of the genotype we found 2 months after birth a similar low percentage of EGFR^{high} cells in both the CA1 (wild type 0.16±0.03 versus *Gdf15*$^{-/-}$ 0.19±0.04) and the DG (wild type 0.06±0.02 versus *Gdf15*$^{-/-}$ 0.08±0.03). We next compared the effect of the genotype in the DG at different postnatal ages. For this purpose, we immunostained postnatal hippocampal sections with antibodies to PHH3 and NeuroD, to visualise immature neuroblasts, doublecortin (DCX), which is expressed in both neuroblasts and

Development (2014) doi:10.1242/dev.096131

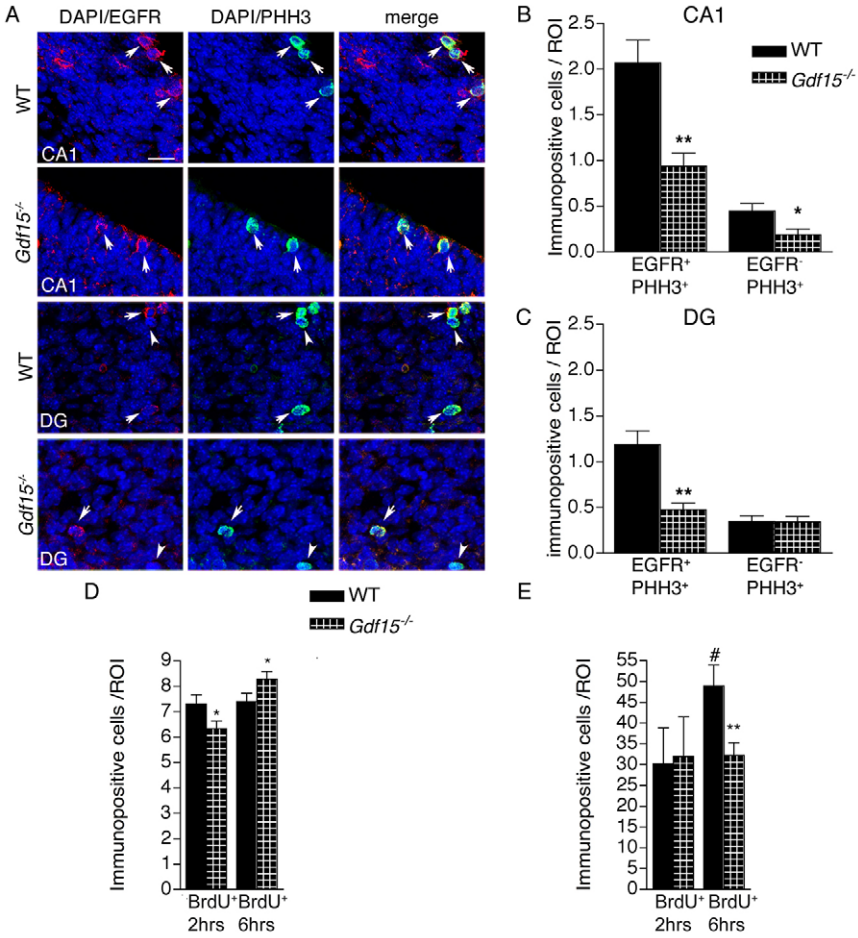

Fig. 5. Reduced proliferation in the E18 *Gdf15*$^{-/-}$ HP. (A) Micrographs illustrating representative examples of EGFR and PHH3 immunoreactivity and DAPI nuclear counterstaining on coronal CA1 and DG sections. Arrows and arrowheads show EGFR$^+$/PHH3$^+$ and PHH3$^+$ cells, respectively. Scale bar: 30 µm. (B,C) Quantitative analysis of the double immunostaining in A within the CA1 (B) and DG (C). (D,E) Quantitative analysis of the number of BrdU$^+$ cells in the CA1 (D) and in the DG (E) 2 and 6 hours after BrdU injection. * and # indicate values that are significantly different from the wild type and from the corresponding cells at 2 hours, respectively. *,$^{\#}P$≤0.05; **,$^{\#\#}P$≤0.01; n=3.

young postmitotic neurons, and calretinin, to identify young postmitotic neurons in the granular layer of the DG (von Bohlen und Halbach, 2011). In 1-month-old mutant animals, the DG contained significantly fewer progenitors and immature neurons than the age-matched wild-type tissue (Fig. 8B). Compared with the wild type, in mutant mice the number of PHH3$^+$ and NeuroD$^+$ precursors were reduced by 46% and 29%, respectively (Fig. 8C), whereas DCX$^+$ and calretinin$^+$ neurons were decreased by 33% and 47%, respectively (Fig. 8D,E). Consistent with previous observations (Kuhn et al., 1996), age led to a decrease in neurogenesis in both genotypes. However, analysis of 3- and 6-month-old animals revealed a progressive reduction of the effect of the genotype on neurogenesis (Fig. 8B-E). At 3 and 6 months, no difference was observed in the number of PHH3$^+$ and NeuroD$^+$ cells between the genotypes. Although the mutant DG of 3-month-old mice still contained 23% and 40% less DCX$^+$ and calretinin$^+$ cells than the wild-type counterpart, at 6 months the densities of DCX$^+$ were not longer significantly affected by the genotype (Fig. 8D,E) and the residual deficit in the number of calretinin$^+$ neurons in the mutant DG also disappeared by 12 months (Fig. 8E and data not shown).

Analysis of BrdU incorporation confirmed that neurogenesis is indeed not altered in 6-month-old mutant mice (supplementary material Fig. S6A-D). Moreover, the genotype did not affect cell death monitored by caspase 3 (supplementary material Fig. S6E-H) and TUNEL labelling (supplementary material Fig. S6I), showing that the absence of an effect of the genotype on neurogenesis in older mice is not a consequence of increased cell death in the wild-type DG.

Taken together, our observations show that *Gdf15* ablation leads to a transient impairment of neurogenesis in the DG of young adult mice. Importantly, differences in proliferation between the genotypes were only observed 1 month after birth, but not at later time points, revealing a correlation between changes in proliferation and EGFR expression also in the postnatal DG.

Neuronal ectopias in the postnatal *Gdf15*$^{-/-}$ HP

We next investigated neuronal distribution in the postnatal CA1. As we had found that in the embryonic HP GDF15 affects the migration of precursors and cells expressing markers of interneurons, we first analysed DCX expression. In both genotypes we observed a similar number of DCX$^+$ immature neurons in the CA1. Consistent with previous observations (Gong et al., 2010; Inta et al., 2008; Yoo et al., 2011), the number of DCX$^+$ cells was low and steeply declined with age (Fig. 9). However, whereas in the HP of 1-month-old wild-type mice DCX$^+$ cells were homogenously distributed in the alveus, in the mutant counterpart they were grouped in clusters (Fig. 9A). Supporting the hypothesis that the effect of the mutation depends on altered EGFR signalling, no difference was observed in the mutant and wild-type alveus with respect to the distribution of DCX cells at 6 months (Fig. 9). Quantification of the various neuronal subpopulations with specific markers across the different CA1 strata revealed no differences in the cell densities of interneurons (calretinin$^+$, calbindin$^+$ or parvalbumin$^+$ neurons) between the genotypes (data not shown). However, we detected a significant increase in the number of CamKIIα$^+$ neurons in the stratum oriens, stratum radiatum and stratum lacunosum-moleculare of the *Gdf15*$^{-/-}$

Development (2014) doi:10.1242/dev.096131

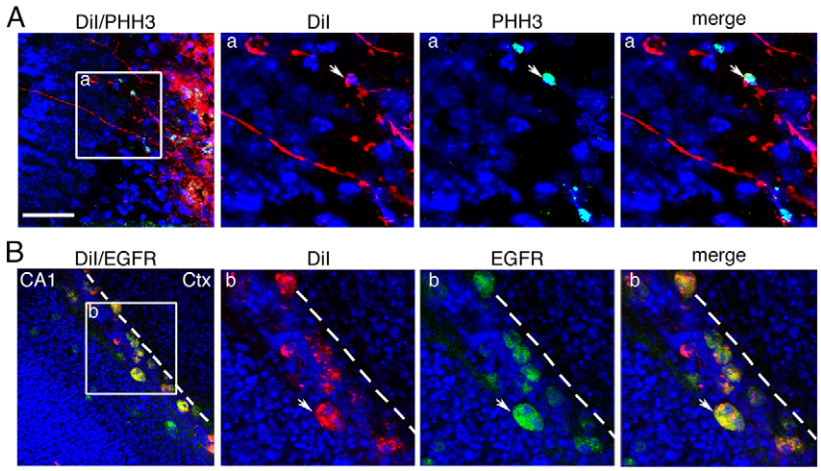

Fig. 6. Characterization of cells migrating within the E18 wild-type CA1. Representative micrographs showing immunoreactivity to PHH3 (A) and EGFR (B) of DiI-labelled cells in organotypic slices maintained *in vitro* for 3 days. Scale bar: 50 µm; 25 µm in higher magnification panels. In B, the dotted line highlights the border between the CA1 and the cortex (CTX). Arrows indicate immunopositive DiI-labelled cells. Higher magnification of the corresponding boxed areas are shown in a and b. Scale bar: 100 µm; 50 µm in higher magnification panels.

CA1 but not in the stratum pyramidale (supplementary material Fig. S7 and data not shown). As the distribution but not the number of DCX^+ cells was altered in the mutant CA1, we concluded that the difference in the number of $CamKII\alpha^+$ cells between the two genotypes reflects an ectopic localization of this cell population rather than a change in proliferation/differentiation. This is consistent with our findings in the developing HP, highlighting a defect in migration within the mutant CA1 region.

DISCUSSION

Here, we provide the first description of the function of GDF15 in the developing telencephalon. We have found that GDF15 affects EGFR signalling and expression in the developing HP, and that lack of GDF15 leads to altered proliferation and migration in this region.

Our data suggest the possibility that the effect of GDF15 on migration and proliferation in the perinatal HP reflects its modulation of EGFR signalling. Consistent with this, we found that *in vitro* the proliferation of mutant precursors was affected only in the presence of exogenous EGF. Mutant precursors also failed to proliferate adequately in response to FGF2 in the presence of additional exogenous EGF, indicating an interaction between EGF and FGF2 signalling. Indeed, we have previously provided evidence that EGF and FGF2 display a synergistic effect in promoting cell proliferation in culture (Ciccolini and Svendsen, 1998). Interestingly, previous studies have highlighted a functional crosstalk between CXCR4, EGF and FGF2 in the regulation of embryonic precursor proliferation *in vitro* (Li et al., 2011). Although the mechanisms underlying the interaction between GDF15 and CXCR4 remain to be investigated, our findings provide now evidence that GDF15 may be part of this complex regulation by promoting EGFR expression in a subset of hippocampal precursors that co-express EGFR and GDF15. In a similar manner, activation of CXCR4 has also been shown to increase EGFR transcript levels in $EGFR^{high}$ cells in the adult SEZ (Kokovay et al., 2010), indicating that this step is a component of the mechanism presiding the fine regulation of EGFR expression and signalling in the neural niche. Interestingly, we found that although both exogenous GDF15 and FGF2 promote the expression of EGFR to control levels in mutant precursors, they cannot rescue their proliferation if EGF is also present in the culture medium. One possible explanation is that exogenous EGF prevents the FGF2 and GDF15 from rescuing EGFR

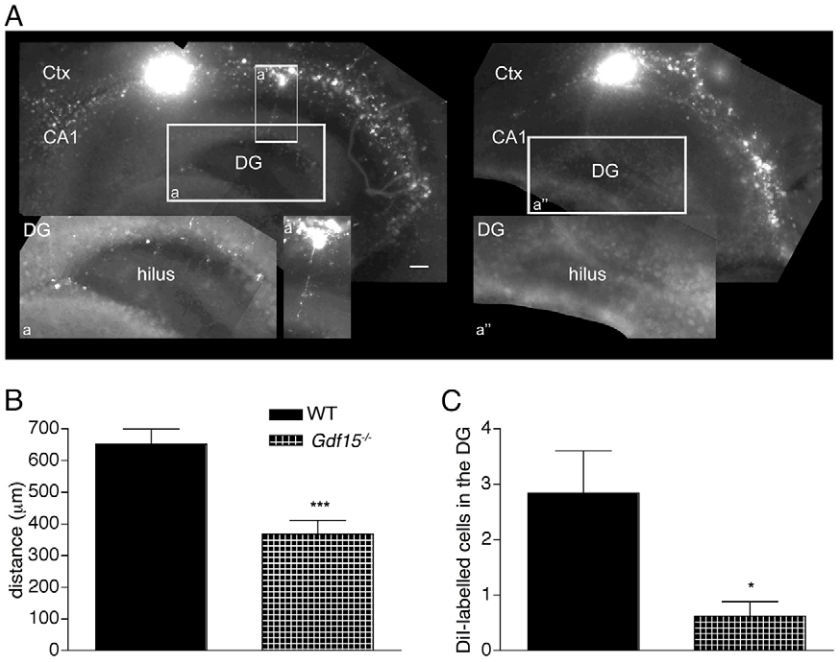

Fig. 7. Impaired migration in the neonatal *Gdf15*$^{-/-}$ CA1. (A) Micrographs illustrating DiI-labelled cells in wild-type (left panels) and *Gdf15*$^{-/-}$ (right panels) organotypic slices. Insets show a higher magnification of the corresponding boxed areas. Scale bar: 200 µm and 100 µm in low and high magnification panels, respectively. (B,C) Quantitative analysis of the distance between the DiI-loaded bead and most distal tangentially migrating cells (B) and of the number of DiI-labelled cells in the DG (C). * indicates values significantly different from the wild type. *P≤0.05; ***P≤0.001; n≥5.

Development (2014) doi:10.1242/dev.096131

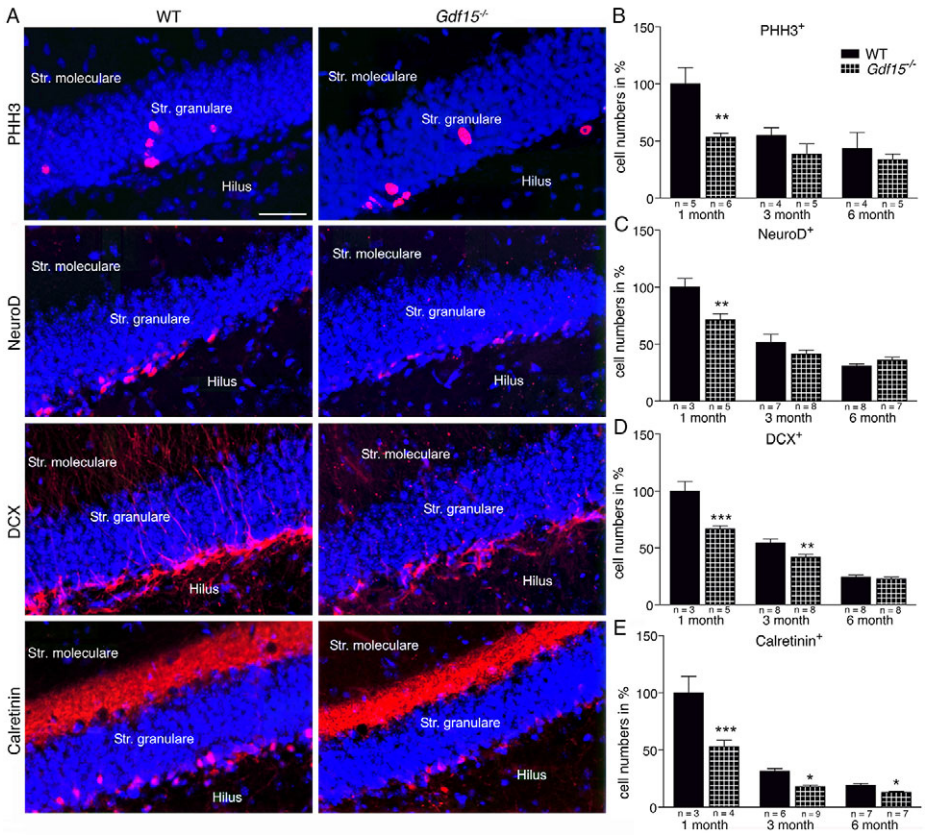

Fig. 8. Impairment of neurogenesis in the perinatal but not in the adult *Gdf15*$^{-/-}$ DG. (A) Representative photomicrographs of coronal sections of 1-month-old wild-type and *Gdf15*$^{-/-}$ DG immunostained as indicated. (B-E) Quantitative analyses of the immunostainings at the indicated ages. * indicates values significantly different from the wild-type counterparts. *P≤0.05; **P≤0.01; ***P≤0.001; n≥3.

expression in mutant precursors. However, we could not directly test this hypothesis as our approach does not allow the detection of EGFR^{high} cells in cultures exposed to EGF.

A strict association between the effect of GDF15 mutation on EGFR signalling and the defect in proliferation was also observed in the developing mutant DG. However, in the mutant CA1 proliferation was decreased in both EGFR$^+$ and EGFR$^-$ cells. One possible interpretation of this observation is that, whereas proliferating EGFR$^+$ and EGFR$^-$ cells are lineage related in the CA1, they belong to different lineages in the DG. Indeed, it was found that distinct precursor pools contribute to the establishing of the germinal region in the DG (Martin et al., 2002).

Increases in EGFR expression have also been shown to promote neural precursor migration in the developing and postnatal telencephalon (Aguirre et al., 2005; Burrows et al., 2000; Caric et al., 2001; Ciccolini et al., 2005). The hypothesis that EGFR signalling is involved in the regulation of migration in the HP is also consistent with previous findings showing numerous neuronal ectopias in the HP of EGFR-null mice (Sibilia et al., 1998). In the developing HP, cells migrating from the CA1 towards the DG include tangentially migrating interneurons. This migration peaks prenatally and continues with a progressive decrease postnatally (Inta et al., 2008; Tricoire et al., 2011). We have shown that EGFR cells in the developing CA1 display morphological characteristics of tangentially migrating cells (Carrillo-García et al., 2010), indicating that EGFR signalling may contribute to migration also in the developing HP. Consistent with this scenario, we observed fewer migrating cells in the perinatal mutant CA1. A defect in migration likely also underlies the abnormal arrangement of DCX$^+$ cells and CamKIIα$^+$ neurons in the adult mutant CA1. However, we could not directly prove this hypothesis as the CamKIIα$^+$ population could not be traced during prenatal development because CamKIIα is expressed only by postnatal hippocampal neurons (Burgin et al., 1990). Interestingly, activation of CXCR4 receptor is also essential in directing interneuron migration in the developing cortex (Stumm et al., 2003). Our findings indicate that, also with respect to migration, GDF15 is involved in regulating the functional interaction between EGFR and CXCR4 signalling. Thus, our data establish GDF15 as a novel factor regulating EGFR expression in the perinatal HP, thereby affecting their proliferation and migration in this region.

MATERIALS AND METHODS

Dissection of the tissue

All animal experiments were approved by the Regierungspräsidium Karlsruhe and the local authorities at the University of Heidelberg. Adult and time-mated pregnant (plug day=1.0) C57/Bl6 (Charles River) and *Gdf15* knockout/LacZ knock-in homozygous (*Gdf15*$^{-/-}$) and heterozygous (*Gdf15*$^{+/-}$) mice were sacrificed by increasing CO_2 concentration followed by neck dislocation. Neonatal mice were sacrificed by decapitation.

The *Gdf15*$^{-/-}$ line was generated and genotyped as previously described (Strelau et al., 2009). Wild-type, *Gdf15*$^{-/-}$ and *Gdf15*$^{+/-}$ embryos were obtained by heterozygous matings.

Neural precursor cultures

Dissociated cells were plated in culture medium consisting of Euromed-N basal medium (Euroclone) and 2% B27 (Gibco). Human recombinant EGF (20 ng/ml), FGF2 (10 ng/ml) (Peprotech) and GDF15 (10 ng/ml, R&D) were added as indicated in the text.

Fluorescence-activated cell sorting (FACS)

Cell sorting was performed by means of a FACSAria (Becton Dickinson) as previously described (Ciccolini et al., 2005). Cells were sorted using a FACSAria sorter and a FACSVantage (Becton Dickinson) in ice-cold sorting medium: Euromed-N basal medium/L-15 medium (Gibco) (1:1), penicillin/streptomycin (100 U/ml), L-glutamine (2 mM), DNase (20 U/ml),

Development (2014) doi:10.1242/dev.096131

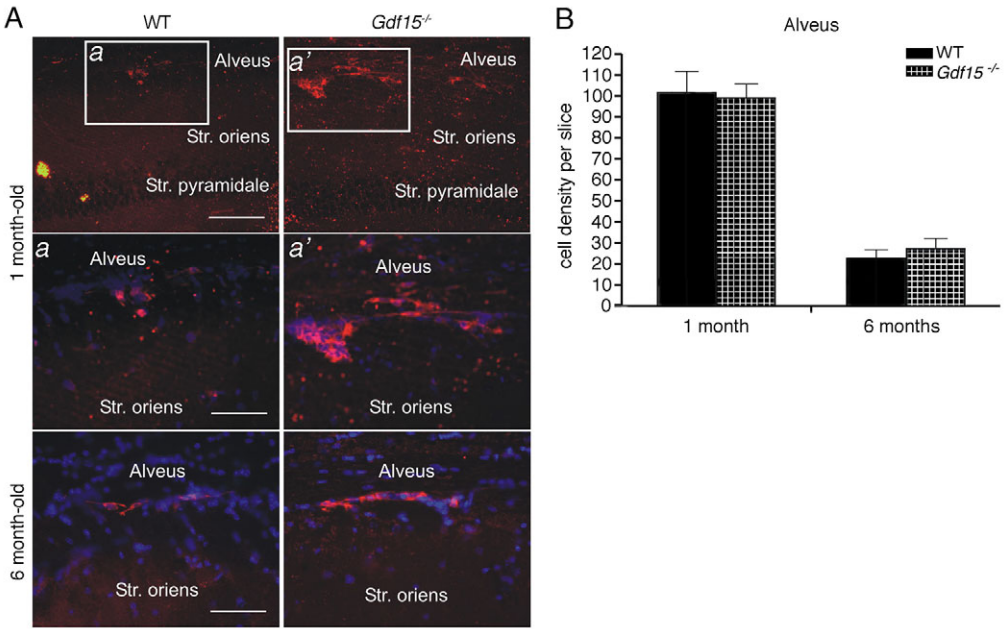

Fig. 9. Abnormal distribution of immature neurons in the CA1 of perinatal but not adult *Gdf15*$^{-/-}$ mice. (A) Micrographs showing DCX^{+} cells (red) in the alveus of 1 (upper and middle row panels) and 6-month-old (lower row panels) wild-type and *Gdf15*$^{-/-}$ mice. Middle row panels show higher magnifications of the corresponding boxed areas. DCX^{+} cells are clustered and dispersed in the 1-month-old *Gdf15*$^{-/-}$ and wild-type tissue, respectively. No significant change instead was observed in the same region at 6 months. Str, stratum. Scale bar: 100 µm in the top panels; 50 µm in the rest. (B) Quantification of the immunostaining shown in A ($n \geq 3$).

B27 (2%), FCS (1%) (BioWhittaker), glucose (0.6%), propidium iodide (1 mg/ml) (all from Sigma) and FGF2 (10 ng/ml). For clonal analysis, cells were plated by FACS-automated cell deposition in 96-well plates (Nunc) containing 50 µl of EGF and FGF2 supplemented culture medium.

EGFR detection

Cells were stained with EGF conjugated to Alexa 488 or Alexa 647 (20 ng/ml, Molecular Probes) immediately after dissection or after being plated at a density of 10^5 cells/ml supplemented with FGF2 in the presence or absence of the CXCR4 inhibitor AMD3100 (10 ng/ml) (Sigma-Aldrich) for 6-24 hours. Sorting gates were set using unstained cells (autofluorescence control), cells stained with PI and cells that had been incubated with EGF culture medium prior to staining with EGF-Alexa (EGF control). EGFR^{low} and EGFR^{high} populations were gated on the basis of a 20-fold decrease or increase in fluorescence levels with respect to the more fluorescent cells in the EGF control.

Prominin detection

Freshly dissociated cells were incubated for 1 hour at 4°C with anti-prominin 1 antibodies conjugated to PE (1:500, MACS) as previously reported (Carrillo-García et al., 2010; Obernier et al., 2011).

β-Galactosidase (LacZ) detection

Dissociated *Gdf15*$^{+/-}$ cells were incubated in a hypo-osmotic solution containing fluorescein di(β-D-galactopyranoside) (FDG, Molecular Probes)/H_2O/sorting medium (1:10:10) at 37°C. After 1 minute, the labelling solution was diluted 10 times with ice-cold sorting medium and kept on ice for 30 minutes before sorting. Sorting gates were set with cells treated with hypo-osmotic solution without FDG.

Quantitative analysis of immunopositive cells

Slices were analysed with a laser scanning confocal microscope (TCS SP2 scanning head and inverted DMIRBE microscope, 40× oil immersion HCX PL APO objective, Leica confocal scan (LCS) software; Leica, Germany). To analyse co-expression, slices were optically sectioned sequentially along the *z*-axis (Δz=0.5 µm). The criterion for double labelling was colocalization of immunoreactivies in three or more consecutive optical sections. Colocalization was further confirmed by analysis of orthogonal projections.

Quantification was obtained from at least three sections/animal and at least three animals. In the embryonic HP the entire hilar field of the DG was counted. In the CA1 and in the SEZ, cells were counted within a squared region of interest with an area of 50 µm^2. For adult neurogenesis, immunopositive cells were counted in sections at comparable rostrocaudal levels, separated from each other by five intervening sections (80 µm in total). Data from the adult DG were expressed as percentage change relative to 1-month-old wild type. Importantly, DAPI nuclear staining revealed no effect of the genotype on cell density in either the embryonic or adult HP.

Antibodies

The following antibodies were used at the indicated dilution: mouse monoclonal α-BrdU, 1:10 (Roche, USA); sheep polyclonal α-EGFR, 1:50; goat polyclonal α-doublecortin, 1:100; rat monoclonal α-nestin, 1:500; rabbit polyclonal α-PHH3, 1:30; rabbit polyclonal α-NeuroD (N19), 1:200; rabbit polyclonal α-Ki67, 1:200; rabbit polyclonal α-CaMK-IIα, 1:100; rabbit polyclonal α-calbindin, 1:200 (all from Abcam, UK); rabbit polyclonal α-PHH3, 1:500 (Upstate, USA); rabbit polyclonal α-PHH3, 1:50 (Santa Cruz, USA); rabbit polyclonal α-GFAP, 1:500; rabbit polyclonal α-calretinin, 1:2000 (all from Chemicon, USA); rabbit polyclonal α-parvalbumin, 1:500 (Immunostar, USA); and rabbit polyclonal, α-GDF15 (1:50, ImmunoGlobe Antikörpertechnik GmbH, Himmelstadt, Germany).

Analysis of cell migration by DiI tracing

Brains were embedded in low melting point agarose (4%, Invitrogen) and 300 µm coronal vibratome sections were cut and transferred onto culture plate inserts (pore size 0.4 µm, Millipore) in culture medium without exogenous growth factors. After 2 hours in the incubator, DiI (Invitrogen) loaded glass beads were carefully delivered with a micropipette just ventral to the corpus callosum in the apical portion of the CA1. After 3 further days, the slices were fixed in PFA (4%) for 4 hours and immunostained. Photomicrographs were taken using an Axioplan 2 imaging microscope equipped with AxioVision software (Zeiss, Germany) and the distance from the external edge of the bead to the most distant DiI-labelled cell along the CA1 was calculated using ImageTool (UTHSCSA; University of Texas, USA) software. Arbitrary units were then converted to µm. For each genotype a minimum of 16 slices derived from at least six different animals were analysed.

Immunohistofluorescence

Embryonic brains were fixed overnight in PFA (4%) at 4°C, transferred into 30% sucrose overnight and embedded in Tissue-Tek for cryopreservation. Coronal slices (16 µm) were cut with a Leica CM3050S cryostat and immunostained as previously described (Ciccolini et al., 2005). For BrdU staining, after permeabilization in NP-40 (0.5%, Sigma), slices were treated with HCl (2 N) and then washed in sodium tetraborate buffer (0.1 M; pH 8.5). After blocking in FCS (5%), slices were incubated overnight at 4°C with primary antibodies. Secondary antibodies conjugated to Cy3 (Jackson

ImmunoResearch) and Alexa 488 (Molecular Probes; Dianova) were used to reveal primary antibody binding.

Postnatal mice were deeply anesthetized and transcardially perfused with heparin (0.25%) followed by PFA (4%). After overnight post-fixation in PFA (4%) at 4°C, coronal brain sections (25 µm) were cut with a vibratome (VT1000E; Leica, Germany). Slices were permeabilized with Triton X-100 (1%). For BrdU detection permeabilized slices were incubated with DNase buffer and with diluted RQ1-DNase. Sections were incubated with the α-BrdU working solution overnight at 4°C.

For GDF15 immunohistofluorescence, slices were processed as previously described (Obernier et al., 2011). 4′,6-Diamidine-2'-phenylindole-dihydrochloride (DAPI, 1:1000) (Roche) was used for nuclear counterstaining.

Real time-PCR

RNA isolation was performed using the TriFast reagent from Peqlab according to the manufacturer's protocol. RNA concentration was measured by optic densitometry using an Eppendorf BioPhotometer and RNA samples were stored at −80°C. Then, cDNA was synthesized by reverse transcription polymerase chain reaction (Promega) and qPCR analysis based on the TaqMan methodology was performed using an ABI Prism 7300 Sequence Detection System (Applied Biosystems). Probes and primer sets were obtained from Applied Biosystems as Assays-on-Demand (AOD). The AOD IDs were: GDF15, Mm00442228-m1; FGF2, Mm00433278-m1; FGFR1, Mm00438923-m1; FGFR2, Mm00438941-m1; 18s, Hs99999901 seconds1; GAPDH, Mm00000015 seconds1; β-Actin, Mm00607939 seconds1. Results were expressed as $2^{-\Delta CT}$, which is an index of the relative amount of mRNA present in each sample.

BrdU labelling

For BrdU analysis we used solutions from the BrdU labelling and detection kit I (Roche Diagnostics GmbH) and followed the manufacturer's protocol. Mice were given BrdU (50 µg/g body weight) by i.p. injection according to the following schedule:

(1) Time mated (E18) pregnant *Gdf15*$^{+/-}$ females were injected once and sacrificed after 2 hours or they were given a second injection 3 hours after the first one and sacrificed after 3 further hours.

(2) Adult animals were injected on 3 consecutive days. Animals were sacrificed two weeks after the last BrdU injection.

Statistical analysis

The means and standard errors of at least three independent experiments were calculated and statistical significance tests (*t*-test or one-way ANOVA, followed by a Bonferroni Post-hoc test) were performed using Prism 4.03 (GraphPad, USA). Calculated *P*-values are indicated in the figure as follows: * and $^{\#}$, $P \leq 0.05$; ** and $^{\#\#}$, $P \leq 0.01$; *** and $^{\#\#\#}$, $P \leq 0.001$.

Acknowledgements

We thank G. Bendner for excellent technical assistance.

Competing interests

The authors declare no competing financial interests.

Author contributions

C.C.-G. and S.P. performed most of the analysis in the embryonic and adult brain, respectively. I.K.S. performed GDF15 immunostaining and analysis of *Egfr* transcripts in sorted cells. J.S. generated the *Ggdf15*$^{-/-}$ mice. C.M. assisted with the experiments. G.H.-W. operated the FACS. K.U. conceived the study. O.v.B.u.H. designed the analysis of adult neurogenesis. F.C. designed the analysis of the embryonic brain, coordinated the experiments and wrote the manuscript.

Funding

F.C., C.C.-G., C.M., G.H.-W. and I.K.S. acknowledge the Landesstiftung Baden-Württemberg for its support. J.S., S.P., K.U. and O.v.B.u.H. acknowledge the Deutsche Forschungsgemeinschaft (UN34/23-1, STR 616/1-4, SFB 636/A5). Deposited in PMC for immediate release.

Supplementary material

Supplementary material available online at
http://dev.biologists.org/lookup/suppl/doi:10.1242/dev.096131/-/DC1

References

Aguirre, A., Rizvi, T. A., Ratner, N. and Gallo, V. (2005). Overexpression of the epidermal growth factor receptor confers migratory properties to nonmigratory postnatal neural progenitors. *J. Neurosci.* **25**, 11092-11106.

Altman, J. and Bayer, S. A. (1990). Mosaic organization of the hippocampal neuroepithelium and the multiple germinal sources of dentate granule cells. *J. Comp. Neurol.* **301**, 325-342.

Beckervordersandforth, R., Tripathi, P., Ninkovic, J., Bayam, E., Lepier, A., Stempfhuber, B., Kirchhoff, F., Hirrlinger, J., Haslinger, A., Lie, D. C. et al. (2010). In vivo fate mapping and expression analysis reveals molecular hallmarks of prospectively isolated adult neural stem cells. *Cell Stem Cell* **7**, 744-758.

Becq, H., Jorquera, I., Ben-Ari, Y., Weiss, S. and Represa, A. (2005). Differential properties of dentate gyrus and CA1 neural precursors. *J. Neurobiol.* **62**, 243-261.

Böttner, M., Suter-Crazzolara, C., Schober, A. and Unsicker, K. (1999). Expression of a novel member of the TGF-beta superfamily, growth/differentiation factor-15/macrophage-inhibiting cytokine-1 (GDF-15/MIC-1) in adult rat tissues. *Cell Tissue Res.* **297**, 103-110.

Burgin, K. E., Waxham, M. N., Rickling, S., Westgate, S. A., Mobley, W. C. and Kelly, P. T. (1990). In situ hybridization histochemistry of Ca2+/calmodulin-dependent protein kinase in developing rat brain. *J. Neurosci.* **10**, 1788-1798.

Burrows, R. C., Lillien, L. and Levitt, P. (2000). Mechanisms of progenitor maturation are conserved in the striatum and cortex. *Dev. Neurosci.* **22**, 7-15.

Cameron, H. A., Woolley, C. S., McEwen, B. S. and Gould, E. (1993). Differentiation of newly born neurons and glia in the dentate gyrus of the adult rat. *Neuroscience* **56**, 337-344.

Caric, D., Raphael, H., Viti, J., Feathers, A., Wancio, D. and Lillien, L. (2001). EGFRs mediate chemotactic migration in the developing telencephalon. *Development* **128**, 4203-4216.

Carrillo-García, C., Suh, Y., Obernier, K., Hölzl-Wenig, G., Mandl, C. and Ciccolini, F. (2010). Multipotent precursors in the anterior and hippocampal subventricular zone display similar transcription factor signatures but their proliferation and maintenance are differentially regulated. *Mol. Cell. Neurosci.* **44**, 318-329.

Cesetti, T., Obernier, K., Bengtson, C. P., Fila, T., Mandl, C., Hölzl-Wenig, G., Wörner, K., Eckstein, V. and Ciccolini, F. (2009). Analysis of stem cell lineage progression in the neonatal subventricular zone identifies EGFR+/NG2- cells as transit-amplifying precursors. *Stem Cells* **27**, 1443-1454.

Cesetti, T., Fila, T., Obernier, K., Bengtson, C. P., Li, Y., Mandl, C., Hölzl-Wenig, G. and Ciccolini, F. (2011). GABAA receptor signaling induces osmotic swelling and cell cycle activation of neonatal prominin+ precursors. *Stem Cells* **29**, 307-319.

Chechneva, O., Dinkel, K., Schrader, D. and Reymann, K. G. (2005). Identification and characterization of two neurogenic zones in interface organotypic hippocampal slice cultures. *Neuroscience* **136**, 343-355.

Choe, Y. and Pleasure, S. J. (2012). Wnt signaling regulates intermediate precursor production in the postnatal dentate gyrus by regulating CXCR4 expression. *Dev. Neurosci.* **34**, 502-514.

Ciccolini, F. (2001). Identification of two distinct types of multipotent neural precursors that appear sequentially during CNS development. *Mol. Cell. Neurosci.* **17**, 895-907.

Ciccolini, F. and Svendsen, C. N. (1998). Fibroblast growth factor 2 (FGF-2) promotes acquisition of epidermal growth factor (EGF) responsiveness in mouse striatal precursor cells: identification of neural precursors responding to both EGF and FGF-2. *J. Neurosci.* **18**, 7869-7880.

Ciccolini, F. and Svendsen, C. N. (2001). Neurotrophin responsiveness is differentially regulated in neurons and precursors isolated from the developing striatum. *J. Mol. Neurosci.* **17**, 25-33.

Ciccolini, F., Mandl, C., Hölzl-Wenig, G., Kehlenbach, A. and Hellwig, A. (2005). Prospective isolation of late development multipotent precursors whose migration is promoted by EGFR. *Dev. Biol.* **284**, 112-125.

Ehninger, D. and Kempermann, G. (2008). Neurogenesis in the adult hippocampus. *Cell Tissue Res.* **331**, 243-250.

Gong, J., Liu, W., Dong, J., Wang, Y., Xu, H., Wei, W., Zhong, J., Xi, Q. and Chen, J. (2010). Developmental iodine deficiency and hypothyroidism impair neural development in rat hippocampus: involvement of doublecortin and NCAM-180. *BMC Neurosci.* **11**, 50.

Inta, D., Alfonso, J., von Engelhardt, J., Kreuzberg, M. M., Meyer, A. H., van Hooft, J. A. and Monyer, H. (2008). Neurogenesis and widespread forebrain migration of distinct GABAergic neurons from the postnatal subventricular zone. *Proc. Natl. Acad. Sci. USA* **105**, 20994-20999.

Kokovay, E., Goderie, S., Wang, Y., Lotz, S., Lin, G., Sun, Y., Roysam, B., Shen, Q. and Temple, S. (2010). Adult SVZ lineage cells home to and leave the vascular niche via differential responses to SDF1/CXCR4 signaling. *Cell Stem Cell* **7**, 163-173.

Kuhn, H. G., Dickinson-Anson, H. and Gage, F. H. (1996). Neurogenesis in the dentate gyrus of the adult rat: age-related decrease of neuronal progenitor proliferation. *J. Neurosci.* **16**, 2027-2033.

Li, G. and Pleasure, S. J. (2005). Morphogenesis of the dentate gyrus: what we are learning from mouse mutants. *Dev. Neurosci.* **27**, 93-99.

Li, M., Chang, C. J., Lathia, J. D., Wang, L., Pacenta, H. L., Cotleur, A. and Ransohoff, R. M. (2011). Chemokine receptor CXCR4 signaling modulates the growth factor-induced cell cycle of self-renewing and multipotent neural progenitor cells. *Glia* **59**, 108-118.

Lillien, L. and Raphael, H. (2000). BMP and FGF regulate the development of EGF-responsive neural progenitor cells. *Development* **127**, 4993-5005.

Maric, D., Fiorio Pla, A., Chang, Y. H. and Barker, J. L. (2007). Self-renewing and differentiating properties of cortical neural stem cells are selectively regulated by

basic fibroblast growth factor (FGF) signaling via specific FGF receptors. *J. Neurosci.* **27**, 1836-1852.
Martin, L. A., Tan, S. S. and Goldowitz, D. (2002). Clonal architecture of the mouse hippocampus. *J. Neurosci.* **22**, 3520-3530.
Nakatomi, H., Kuriu, T., Okabe, S., Yamamoto, S., Hatano, O., Kawahara, N., Tamura, A., Kirino, T. and Nakafuku, M. (2002). Regeneration of hippocampal pyramidal neurons after ischemic brain injury by recruitment of endogenous neural progenitors. *Cell* **110**, 429-441.
Navarro-Quiroga, I., Hernandez-Valdes, M., Lin, S. L. and Naegele, J. R. (2006). Postnatal cellular contributions of the hippocampus subventricular zone to the dentate gyrus, corpus callosum, fimbria, and cerebral cortex. *J. Comp. Neurol.* **497**, 833-845.
Obernier, K., Simeonova, I., Fila, T., Mandl, C., Holzl-Wenig, G., Monaghan-Nichols, P. and Ciccolini, F. (2011). Tlx is expressed in both stem cells and transit amplifying progenitors regulating stem cell activation and differentiation in the neonatal lateral subependymal zone. *Stem Cells* **29**, 1415-1426.
Okano, H. J., Pfaff, D. W. and Gibbs, R. B. (1996). Expression of EGFR-, p75NGFR-, and PSTAIR (cdc2)-like immunoreactivity by proliferating cells in the adult rat hippocampal formation and forebrain. *Dev. Neurosci.* **18**, 199-209.
Raballo, R., Rhee, J., Lyn-Cook, R., Leckman, J. F., Schwartz, M. L. and Vaccarino, F. M. (2000). Basic fibroblast growth factor (Fgf2) is necessary for cell proliferation and neurogenesis in the developing cerebral cortex. *J. Neurosci.* **20**, 5012-5023.
Rietze, R., Poulin, P. and Weiss, S. (2000). Mitotically active cells that generate neurons and astrocytes are present in multiple regions of the adult mouse hippocampus. *J. Comp. Neurol.* **424**, 397-408.
Saarimäki-Vire, J., Peltopuro, P., Lahti, L., Naserke, T., Blak, A. A., Vogt Weisenhorn, D. M., Yu, K., Ornitz, D. M., Wurst, W. and Partanen, J. (2007). Fibroblast growth factor receptors cooperate to regulate neural progenitor properties in the developing midbrain and hindbrain. *J. Neurosci.* **27**, 8581-8592.
Santa-Olalla, J. and Covarrubias, L. (1999). Basic fibroblast growth factor promotes epidermal growth factor responsiveness and survival of mesencephalic neural precursor cells. *J. Neurobiol.* **40**, 14-27.
Schober, A., Böttner, M., Strelau, J., Kinscherf, R., Bonaterra, G. A., Barth, M., Schilling, L., Fairlie, W. D., Breit, S. N. and Unsicker, K. (2001). Expression of growth differentiation factor-15/ macrophage inhibitory cytokine-1 (GDF-15/MIC-1) in the perinatal, adult, and injured rat brain. *J. Comp. Neurol.* **439**, 32-45.
Sibilia, M., Steinbach, J. P., Stingl, L., Aguzzi, A. and Wagner, E. F. (1998). A strain-independent postnatal neurodegeneration in mice lacking the EGF receptor. *EMBO J.* **17**, 719-731.
Soriano, E., Del Río, J. A., Martínez, A. and Supèr, H. (1994). Organization of the embryonic and early postnatal murine hippocampus. I. Immunocytochemical characterization of neuronal populations in the subplate and marginal zone. *J. Comp. Neurol.* **342**, 571-595.
Strelau, J., Sullivan, A., Böttner, M., Lingo, P., Falkenstein, E., Suter-Crazzolara, C., Galter, D., Jaszai, J., Krieglstein, K. and Unsicker, K. (2000). Growth/differentiation-15/macrophage inhibitory cytokine-1 is a novel trophic factor for midbrain dopaminergic neurons in vivo. *J. Neurosci.* **20**, 8597-8603
Strelau, J., Strzelczyk, A., Rusu, P., Bendner, G., Wiese, S., Diella, F., Altick, A. L., von Bartheld, C. S., Klein, R., Sendtner, M. et al. (2009). Progressive postnatal motoneuron loss in mice lacking GDF-15. *J. Neurosci.* **29**, 13640-13648.
Stumm, R. K., Zhou, C., Ara, T., Lazarini, F., Dubois-Dalcq, M., Nagasawa, T., Höllt, V. and Schulz, S. (2003). CXCR4 regulates interneuron migration in the developing neocortex. *J. Neurosci.* **23**, 5123-5130.
Tricoire, L., Pelkey, K. A., Erkkila, B. E., Jeffries, B. W., Yuan, X. and McBain, C. J. (2011). A blueprint for the spatiotemporal origins of mouse hippocampal interneuron diversity. *J. Neurosci.* **31**, 10948-10970.
Tucker, M. S., Khan, I., Fuchs-Young, R., Price, S., Steininger, T. L., Greene, G., Wainer, B. H. and Rosner, M. R. (1993). Localization of immunoreactive epidermal growth factor receptor in neonatal and adult rat hippocampus. *Brain Res.* **631**, 65-71.
von Bohlen und Halbach, O. (2011). Immunohistological markers for proliferative events, gliogenesis, and neurogenesis within the adult hippocampus. *Cell Tissue Res.* **345**, 1-19.
Walker, T. L., Wierick, A., Sykes, A. M., Waldau, B., Corbeil, D., Carmeliet, P. and Kempermann, G. (2013). Prominin-1 allows prospective isolation of neural stem cells from the adult murine hippocampus. *J. Neurosci.* **33**, 3010-3024.
Yoo, D. Y., Yoo, K. Y., Choi, J. W., Kim, W., Lee, C. H., Choi, J. H., Park, J. H., Won, M. H. and Hwang, I. K. (2011). Time course of postnatal distribution of doublecortin immunoreactive developing/maturing neurons in the somatosensory cortex and hippocampal CA1 region of C57BL/6 mice. *Cell. Mol. Neurobiol.* **31**, 729-736.

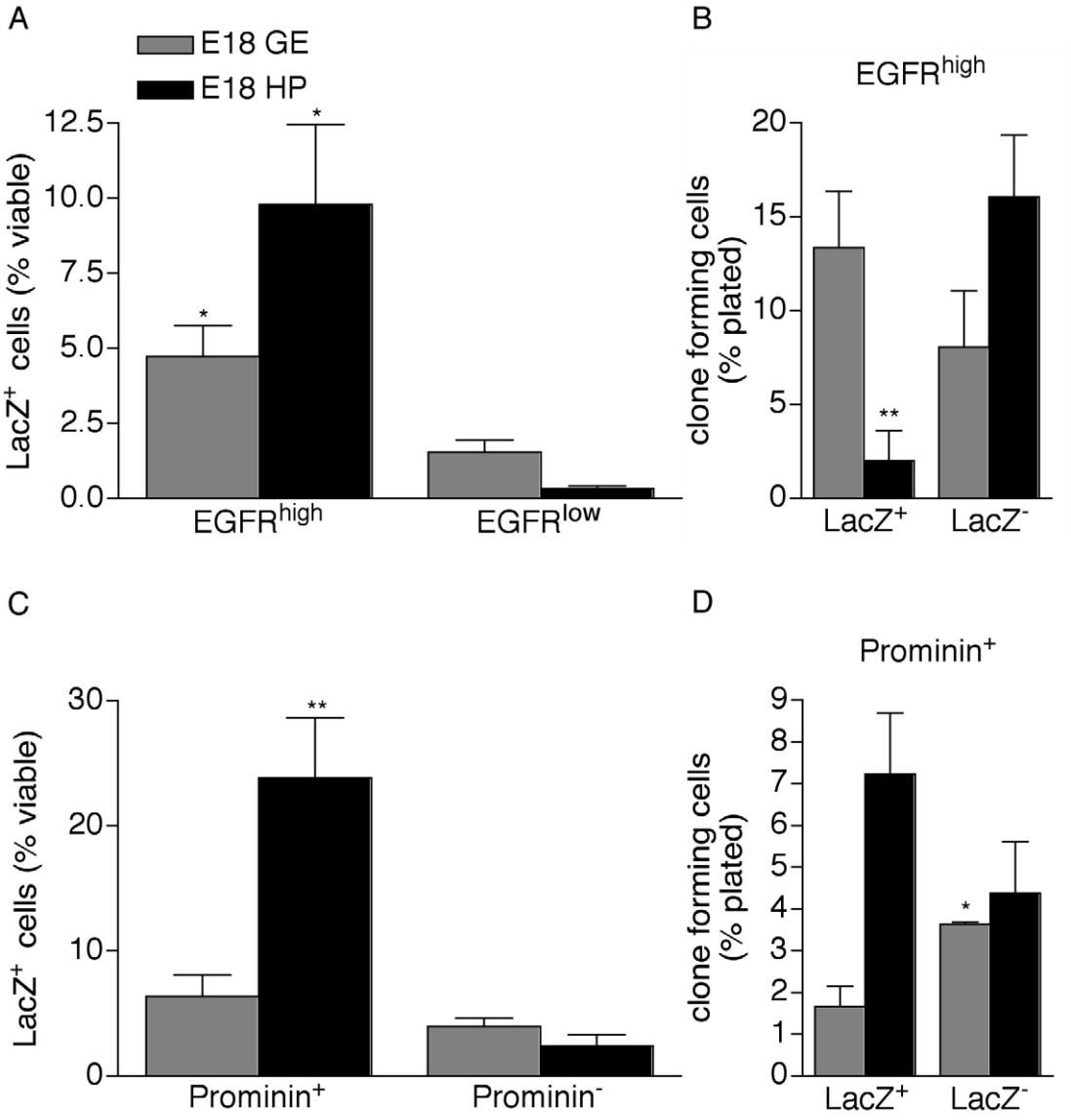

Supplementary Figure 1: In the E18 HP *Gdf15* expressing cells include a subset of neural stem cells. (A and C) Percentage of cells displaying β-galactosidase activity ($LacZ^+$) in the dissociated cells of the E18 *Gdf15*$^{+/-}$ GE and HP sorted according to levels of expression of EGFR (A) and Prominin (C). (B and D) Quantitative analysis of the clone-forming activity in cells sorted on the EGFR (B) or Prominin (D) expression and LacZ activity. * indicate significantly different from the corresponding $EGFR^{low}$ (A), $Prominin^-$ (C), $LacZ^-$ (B, D) population. *: $P \leq 0.05$; ** $P \leq 0.01$, $n \geq 5$.

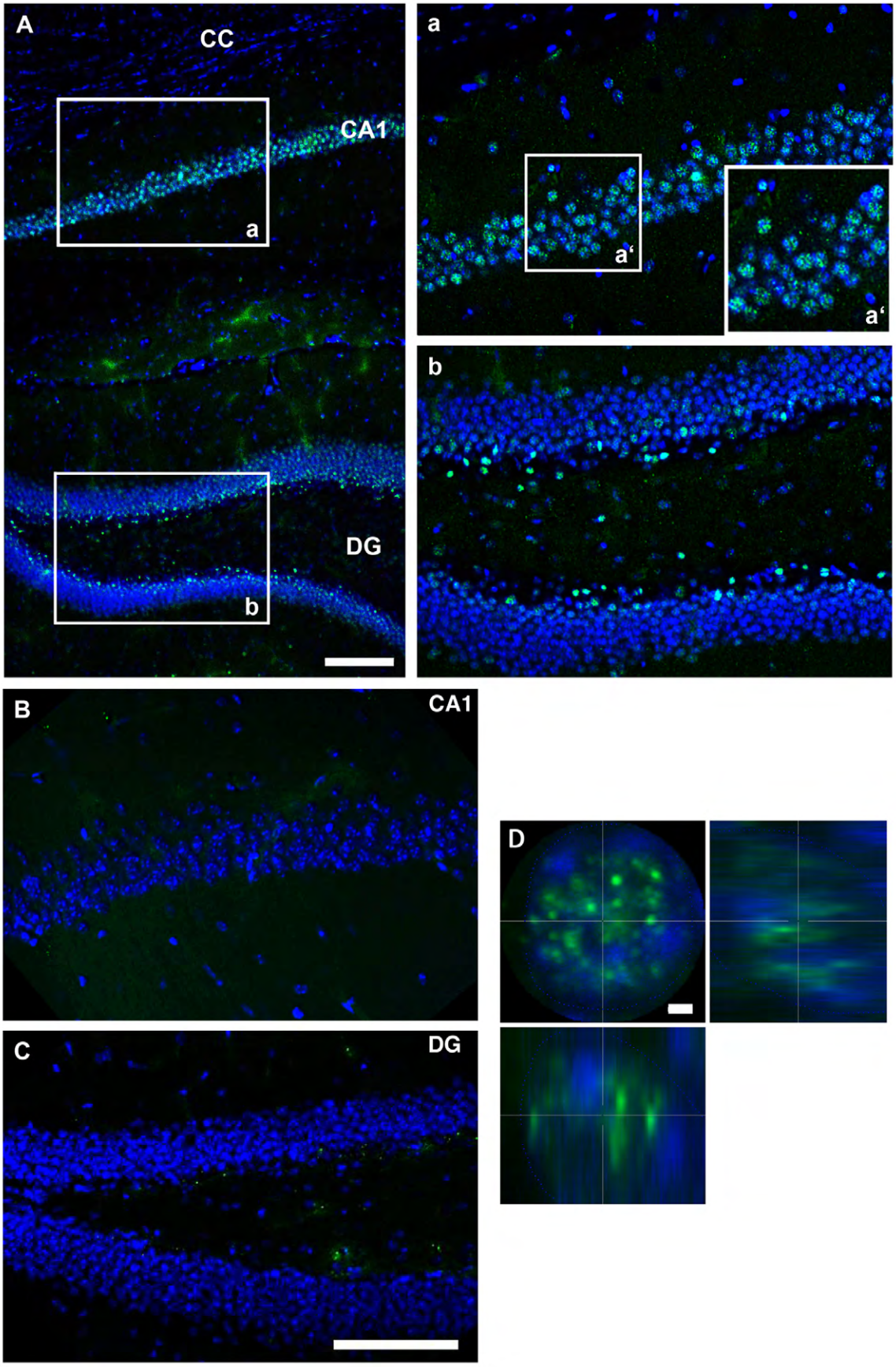

Supplementary Figure 2: Expression of GDF-15 protein in the adult HP. Representative photomicrographs illustrating coronal sections of the WT (A) and *Gdf15*$^{-/-}$ (B, C) CA1 (A, B) and DG (A, C) after immunostaining with α-GDF-15 (green fluorescence). (a), (b) and (a') show higher magnifications of the boxed areas in (Aa), (Ab) and (a), respectively. DAPI counterstaining of the nuclei is shown in blue. Orthogonal projections of a GDF-15^{+} nucleus were obtained at a magnification of ~200x to assess localization (D). Scale bars are 100 µm in A-C and 1 µm in D.

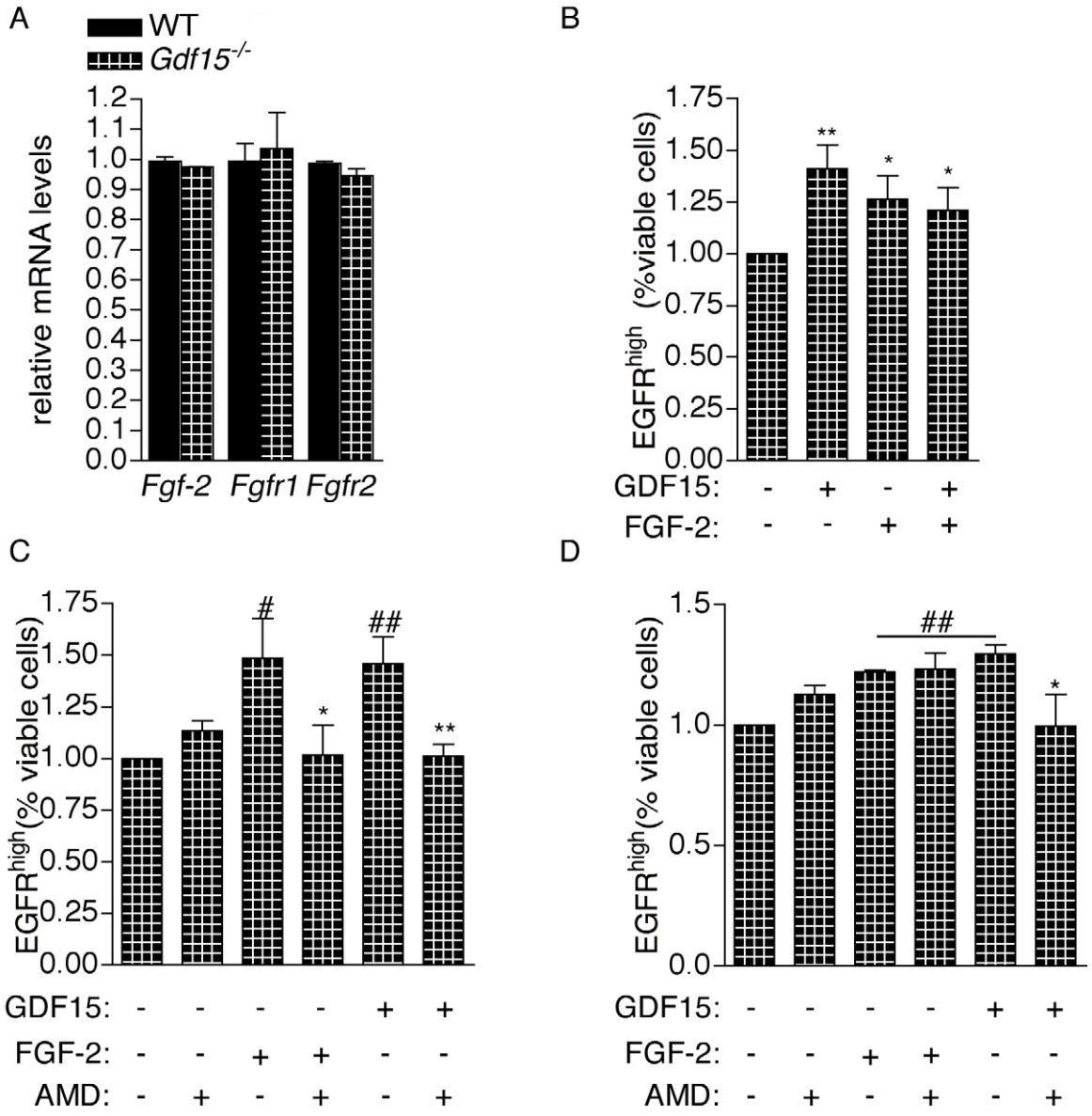

Supplementary Figure 3: GDF-15 modulates EGFR expression independently of FGF signalling. (A) Comparison of *Fgf-2*, *Fgfr1* and *Fgfr2* mRNA levels relative to *Gapdh* and β-Actin mRNAs in WT and *Gdf15*$^{-/-}$ HP. (B-D) Quantitative analysis of the number of EGFR^{high} cells isolated from the E18 *Gdf15*$^{-/-}$ HP after incubation for 6 (B-C) and 24 (D) hours in the presence and/or absence of exogenous growth factors and CXCR-4 blocker AMD3100 as indicated. * denotes significantly different from control cells not exposed to growth factors (B) and counterparts not treated with AMD3100 (C, D). # denotes significantly different from cells exposed to neither growth factors nor AMD3100.*,#: $P \leq 0.05$. **,##: $P \leq 0.01$; $n \geq 3$.

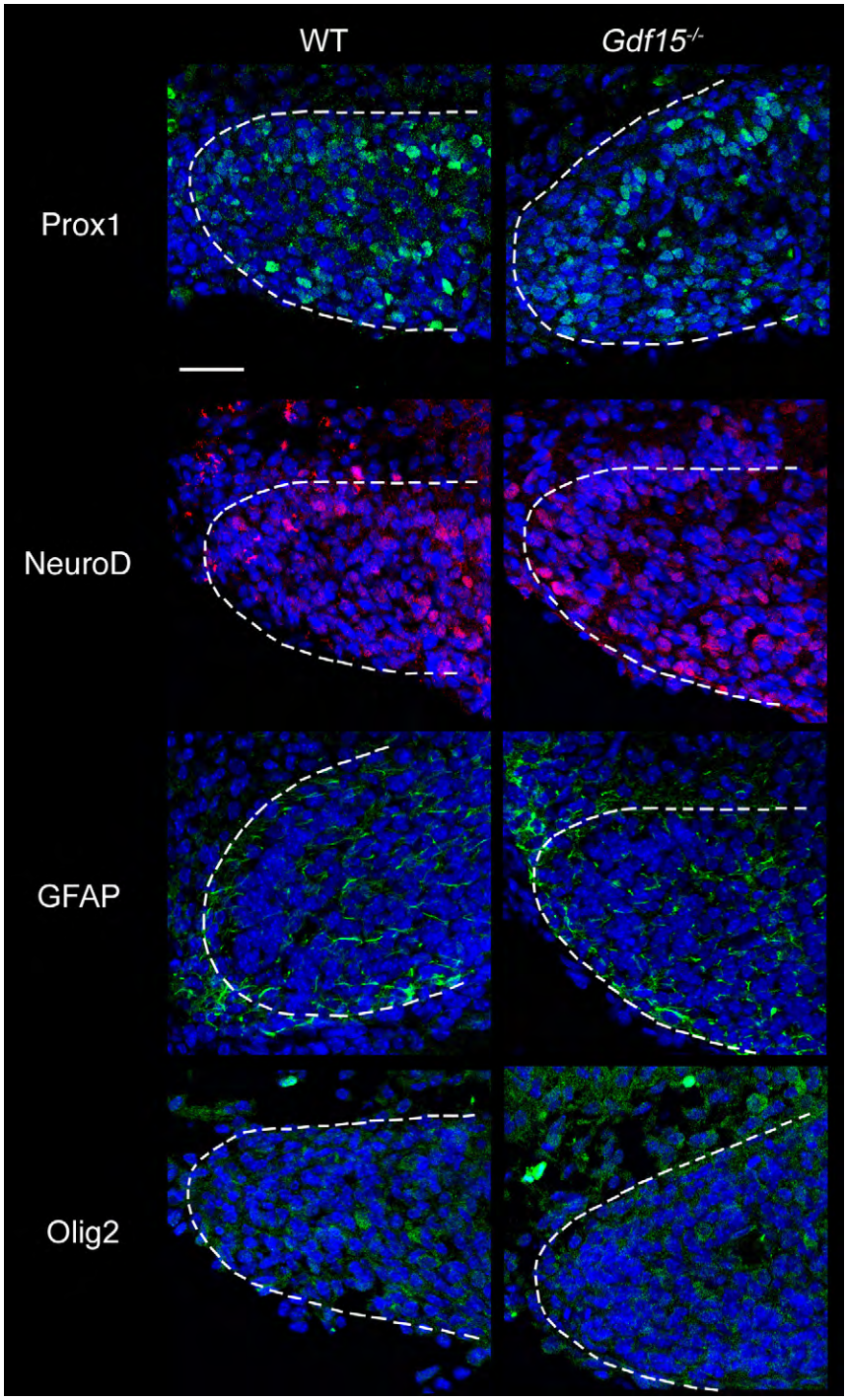

Supplementary Figure 4: Qualitative analysis of the expression of the indicated antigens in E18 WT and *Gdf15*$^{-/-}$ HP by immunostaining. DAPI counterstaining of the nuclei is shown in blue. Scale bar is 37.5mm.

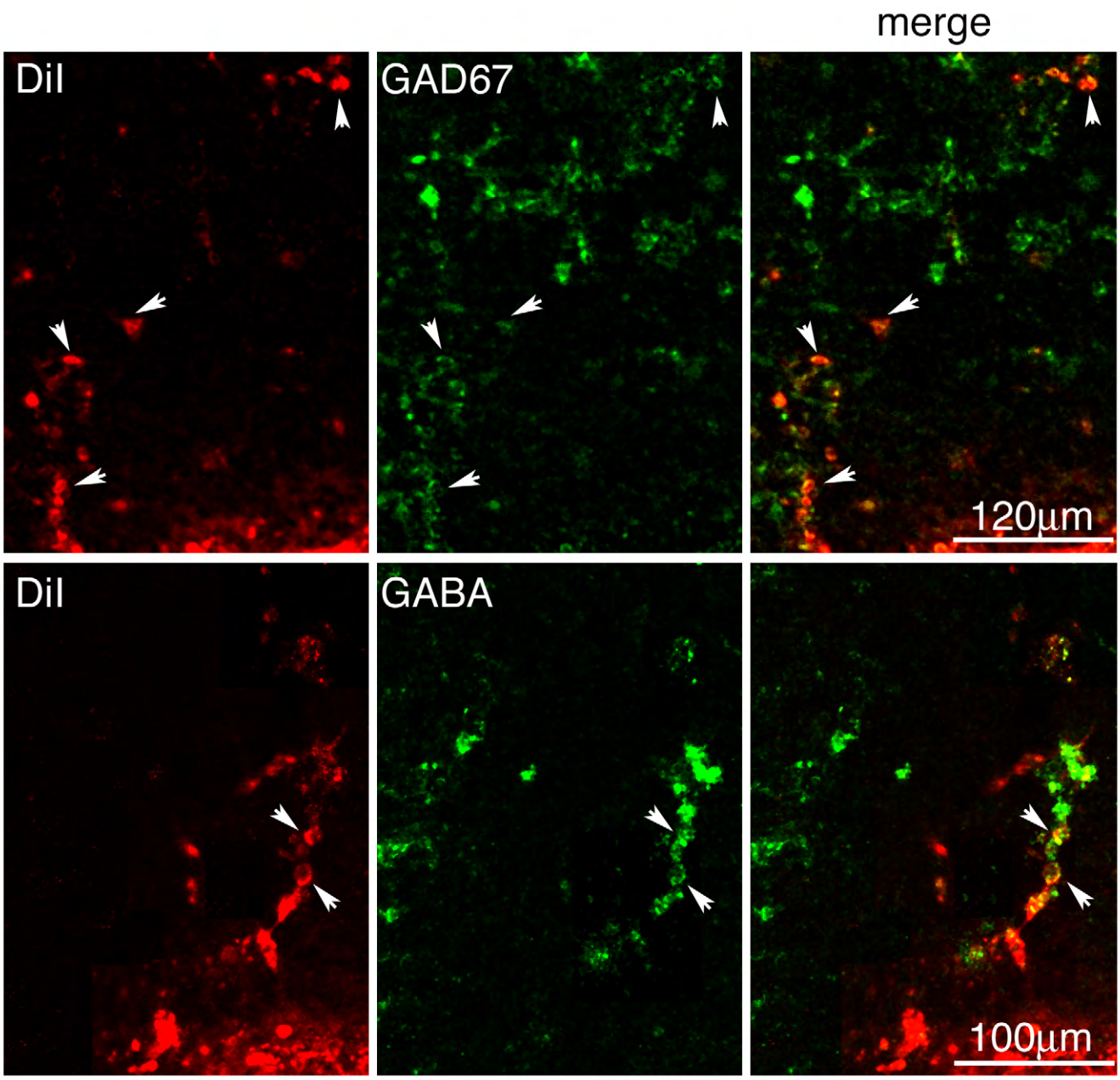

Supplementary Figure 5: Representative micrographs showing immunoreactivity to GAD67 and GABA antibodies of DiI-labelled cells in the CA1 in organotypic slices of the E18 HP that had been cultured *in vitro* for 3 days.

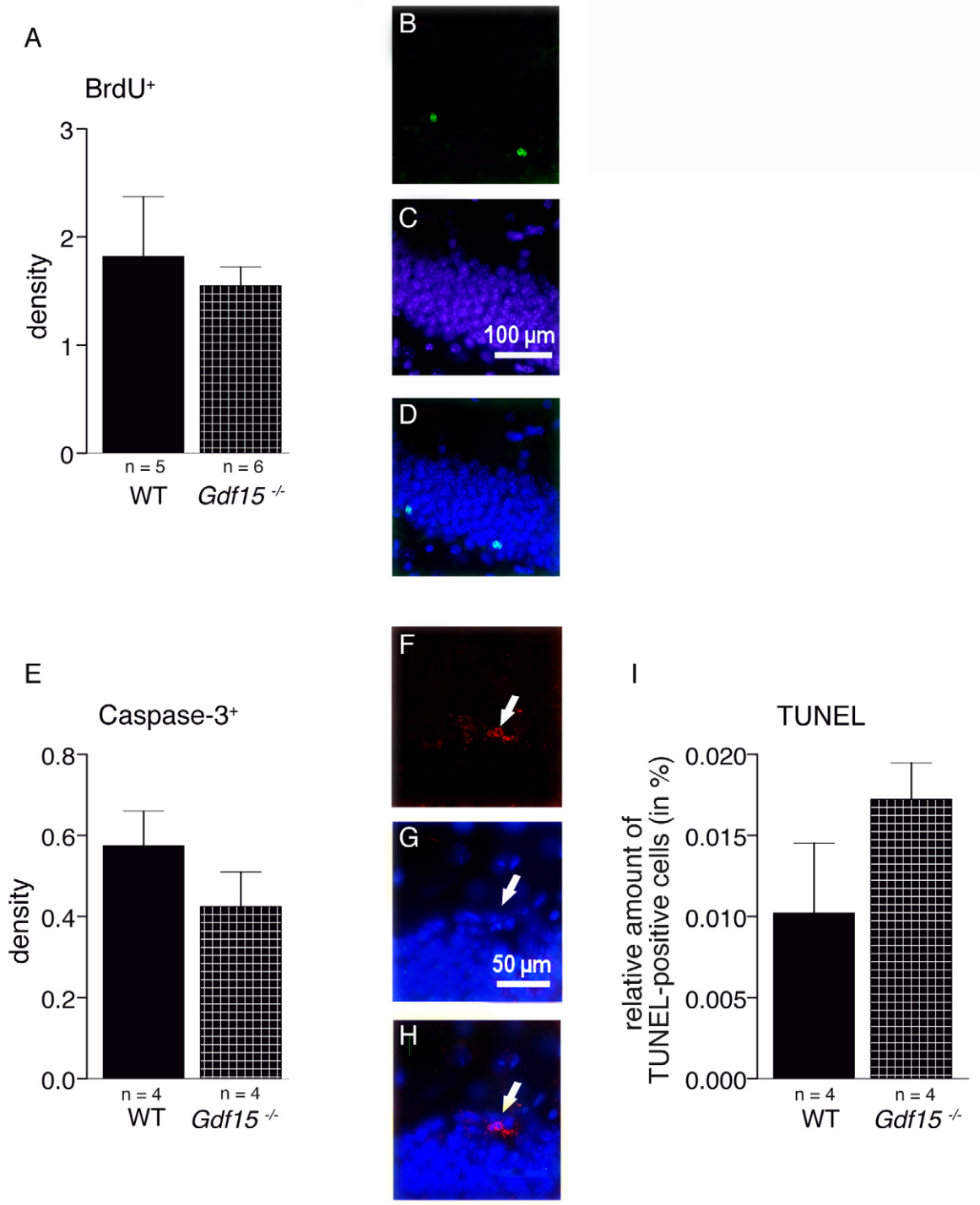

Supplementary Figure 6: Proliferation and cell death in the HP of 6 month-old mice are not affected by the genotype. (A) Quantitative analysis of the number of BrdU immunopositive cells in WT and *Gdf15*$^{-/-}$ in the DG of 6 month-old animals. Data are expressed as means of the number of cells per slice. (B-D) representative images of BrdU-labelled cells (B) DAPI counterstained of nuclei (C) and merge (D) within the DG. (E) Densities of activated caspase 3 positive cells were not altered in 6 month-old *Gdf15*$^{-/-}$ animals, indicating no effect of the genotype on apoptosis. (F-H) representative images of activated caspase-3-labelled cells (F) DAPI cell nuclei (G) and merge (H) within the DG. (I) TUNEL-experiments also demonstrate no significant change in the rate of apoptosis.

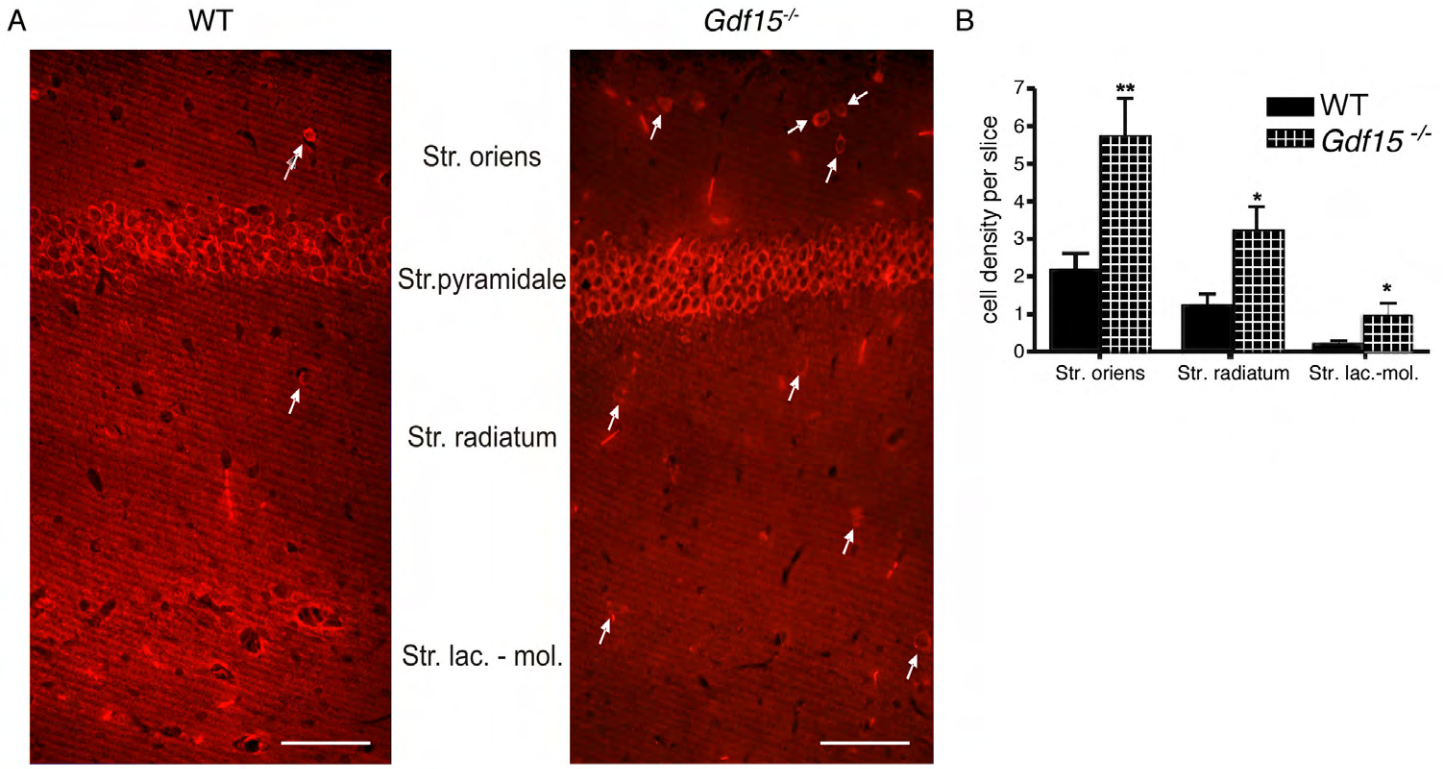

Supplementary Figure 7: Adult *Gdf15*$^{-/-}$ mice show neuronal alteration within the hippocampal area CA1. (A) Representative photomicrographs showing immunostaining for CamKIIα in the CA1 of WT and *Gdf15*$^{-/-}$ 6 month-old animals. Arrows point to some CamKIIα^{+} cells. Scale bar is 100 µm. (B) Quantification of the cell densities of CamKIIα^{+} cells in different layers of the CA1 region. * indicate significantly different from WT counterpart values. *: P≤0.05; **P:≤0.01; n≥3.